Author Contributions:

Conceptualization: William R. Wieder, Emily Kyker-Snowman, A. Stuart Grandy
Data curation: William R. Wieder
Formal analysis: William R. Wieder, Katherine S. Rocci
Funding acquisition: William R. Wieder
Investigation: William R. Wieder, Melannie D. Hartman, Emily Kyker-

Simulating Global Terrestrial Carbon and Nitrogen Biogeochemical Cycles With Implicit and Explicit Representations of Soil Microbial Activity

William R. Wieder[1,2] ![ORCID], Melannie D. Hartman[1,3] ![ORCID], Emily Kyker-Snowman[4] ![ORCID], Brooke Eastman[5] ![ORCID], Katerina Georgiou[6] ![ORCID], Derek Pierson[7], Katherine S. Rocci[2,8] ![ORCID], and A. Stuart Grandy[9,10]

[1]Climate and Global Dynamics Laboratory, National Center for Atmospheric Research, Boulder, CO, USA, [2]Institute of Arctic and Alpine Research, University of Colorado, Boulder, CO, USA, [3]Natural Resource Ecology Laboratory, Colorado State University, Fort Collins, CO, USA, [4]Carbon Direct, New York, NY, USA, [5]Division of Forestry and Natural Resources, West Virginia University, Morgantown, WV, USA, [6]Physical and Life Sciences Directorate, Lawrence Livermore National Laboratory, Livermore, CA, USA, [7]Rocky Mountain Research Station, United States Forest Service, Boise, ID, USA, [8]Institute for Global Change Biology, University of Michigan, Ann Arbor, MI, USA, [9]Department of Natural Resources and the Environment, University of New Hampshire, Durham, NH, USA, [10]Center of Soil Biogeochemistry and Microbial Ecology, University of New Hampshire, Durham, NH, USA

Abstract Nutrient limitation is widespread in terrestrial ecosystems. Accordingly, representations of nitrogen (N) limitation in land models typically dampen rates of terrestrial carbon (C) accrual, compared with C-only simulations. These previous findings, however, rely on soil biogeochemical models that implicitly represent microbial activity and physiology. Here we present results from a biogeochemical model testbed that allows us to investigate how an explicit versus implicit representation of soil microbial activity, as represented in the MIcrobial-MIneral Carbon Stabilization (MIMICS) and Carnegie-Ames-Stanford Approach (CASA) soil biogeochemical models, respectively, influence plant productivity, and terrestrial C and N fluxes at initialization and over the historical period. When forced with common boundary conditions, larger soil C pools simulated by the MIMICS model reflect longer inferred soil organic matter (SOM) turnover times than those simulated by CASA. At steady state, terrestrial ecosystems experience greater N limitation when using the MIMICS-CN model, which also increases the inferred SOM turnover time. Over the historical period, however, warming-induced acceleration of SOM decomposition over high latitude ecosystems increases rates of N mineralization in MIMICS-CN. This reduces N limitation and results in faster rates of vegetation C accrual. Moreover, as SOM stoichiometry is an emergent property of MIMICS-CN, we highlight opportunities to deepen understanding of sources of persistent SOM and explore its potential sensitivity to environmental change. Our findings underscore the need to improve understanding and representation of plant and microbial resource allocation and competition in land models that represent coupled biogeochemical cycles under global change scenarios.

Plain Language Summary Nitrogen limitation of terrestrial ecosystems is common, and crates feedbacks between aboveground and belowground biogeochemical cycles. We present a novel analysis looking at how the explicit versus implicit representation of soil microbial activity influences ecosystem carbon and nitrogen fluxes in a global biogeochemical model. With the microbial explicit model, MIcrobial-MIneral Carbon Stabilization-carbon-nitrogen, we found increases in the inferred turnover time of soil organic matter (SOM) that were caused by plant-soil feedbacks from nitrogen limitation of plant productivity. Over the historical period, we found that warming-induced acceleration of SOM decomposition resulted in higher rates of nitrogen mineralization and vegetation biomass accrual. Collectively, these findings present new opportunities to investigate plant-soil interactions with a model that explicitly represents microbial decomposers.

1. Introduction

Terrestrial ecosystems are characterized by widespread nutrient limitation, especially of nitrogen (N; Elser et al., 2007; LeBauer & Treseder, 2008). These limitations fundamentally shape ecosystem feedbacks between above- and belowground processes (Wardle et al., 2004). Plant investment in belowground carbon (C) allocation and nutrient acquisition strategies influences soil biogeochemical cycles, notably through the formation and decomposition of soil organic matter (SOM; Averill et al., 2014). Moreover, microbial biomass is a major driver

Snowman, Brooke Eastman, Katerina Georgiou, Derek Pierson, A. Stuart Grandy
Methodology: William R. Wieder, Melannie D. Hartman, Emily Kyker-Snowman, Brooke Eastman, A. Stuart Grandy
Project administration: William R. Wieder
Resources: William R. Wieder, A. Stuart Grandy
Software: William R. Wieder, Melannie D. Hartman, Brooke Eastman
Supervision: William R. Wieder
Validation: William R. Wieder, Brooke Eastman
Visualization: William R. Wieder
Writing – original draft: William R. Wieder
Writing – review & editing: William R. Wieder, Melannie D. Hartman, Emily Kyker-Snowman, Brooke Eastman, Katerina Georgiou, Derek Pierson, Katherine S. Rocci, A. Stuart Grandy

of nitrogen mineralization rates (Li et al., 2019). Thus, shifting patterns of plant and microbial stoichiometry, allocation, and activity in response to global change drivers will likely influence terrestrial ecosystem responses to climate change (Wieder, Cleveland, et al., 2015; Zaehle et al., 2015). Accurately capturing these ecological processes and plant-soil feedbacks in models that are used for climate change projections remains a challenge.

Part of this uncertainty reflects gaps in our theoretical understanding of plant-soil feedbacks and their influence on nutrient availability. Notably, emerging theories emphasize the importance of microbial-mineral interactions that govern SOM persistence (Cotrufo et al., 2013; Lehmann et al., 2020; Lehmann & Kleber, 2015). Yet, explicit representations of microbial activity, microbial functional traits, and the protection of soil C via organo-mineral interactions are notably absent from models that are used to project C cycle-climate feedbacks (Todd-Brown et al., 2013). The introduction of global-scale, microbial explicit soil biogeochemical models has opened new lines of research (Huang et al., 2018; Sulman et al., 2014; Wieder et al., 2013; Wieder, Grandy, et al., 2015), but much of the work to date only focuses on the representation of soil C biogeochemistry. Results from ecosystem-scale simulations show the potential for models that explicitly simulate microbial-mineral interactions to advance understanding of coupled carbon-nitrogen (CN) dynamics (Eastman et al., 2023; Kyker-Snowman et al., 2020; Thum et al., 2019; G. Wang et al., 2020; Y. Zhang et al., 2021). Now, application of microbial explicit CN soil models is feasible at global scales (Y. Huang et al., 2021; Sulman et al., 2019), although to date analyses of global terrestrial C and N dynamics from this class of models are sparse.

The current generation of global models consistently show that representing terrestrial nutrient limitation dampens terrestrial ecosystem responses to elevated CO_2 (Thornton et al., 2007; Y. P. Wang et al., 2010; Zaehle et al., 2010). However, these results come from models that implicitly represent soil microbial activity. Preliminary work with models that explicitly represent microbial activity demonstrate shifts in the timing and magnitude of ecosystem C fluxes, relative to models that make microbial implicit assumptions (Basile et al., 2020; Jian et al., 2021; Wieder et al., 2018, 2019). This suggests that models based on distinct underlying structural assumptions will also generate differences in soil N fluxes that may feedback onto ecosystem productivity and response to global change.

We begin to explore these dynamics by coupling two different soil biogeochemical models that represent C and N biogeochemistry to a common vegetation model. This biogeochemical model testbed allows us to investigate how alternative soil model assumptions, structures, and parameterizations ultimately influence plant productivity and ecosystem C storage. This is one of the first global-scale applications of a microbially explicit model to look at ecosystem C and N responses at initialization and in historical simulations (see also Dunne et al., 2020; Sulman et al., 2019). Our objectives are to describe differences in the underlying assumptions of both microbial explicit and microbial implicit model structures that are applied by the MIcrobial-MIneral Carbon Stabilization (MIMICS; Wieder et al., 2014; Wieder, Grandy, et al., 2015) and Carnegie-Ames-Stanford Approach (CASA; Y. P. Wang et al., 2010) soil biogeochemical models, respectively. Subsequently, we describe global scale patterns of soil biogeochemical states and fluxes that are simulated by MIMICS and CASA under steady-state conditions. Finally, we explore the transient biogeochemical response of terrestrial ecosystems over the historical period and discuss future opportunities for representing CN biogeochemistry with microbial explicit structures in land models.

2. Materials and Methods

2.1. Biogeochemical Model Testbed and Forcing

Simulations presented here build on the C-only version of the biogeochemical model testbed, which couples the CASA vegetation model with the CASA or MIMICS soil biogeochemical models (Wieder et al., 2018, 2019). Additional developments to represent soil CN biogeochemistry in site-level simulations with MIMICS-CN are provided in Kyker-Snowman et al. (2020). Here we present a global application of MIMICS-CN that connects with representation of vegetation nutrient limitation and soil N transformations that are also applied in CASA-CNP (Y. P. Wang et al., 2010). We compare global-scale results of vegetation and soil pools and fluxes from simulations with C-only and CN configurations of both MIMICS and CASA soil biogeochemical models. As this work builds on an extensive body of literature, including ecosystem scale simulations with the biogeochemical model testbed presented by Eastman et al. (2023), we largely highlight modifications that were implemented in the development and evaluation of global scale simulations with MIMICS-CN in the biogeochemical model testbed.

The biogeochemical model testbed requires daily inputs of gross primary production (GPP), air temperature, soil temperature, and soil moisture. We generated these boundary conditions by running a historical simulation of the Community Land Model, version 5, with satellite phenology (CLM5-SP) that was driven with atmospheric forcing from the Global Soil Wetness Program, version 3 (GSWP3, see Lawrence et al., 2019). Our previous work with the biogeochemical model testbed used an older version of CLM (version 4.5) and CRU-NCEP forcing (Wieder et al., 2018). Comparison of CLM model versions and forcing data are described in Lawrence et al. (2019) and Bonan et al. (2019). Daily history files from the nominal two degree-resolution CLM5-SP simulations were processed to generate the required meteorological forcings, or *met* files, that are needed to run the biogeochemical model testbed (see technical documentation in will wieder & melanniehartman, 2023). This processing step involves calculating depth weighted mean daily soil temperature along with volumetric liquid and frozen soil water content for the top six soil layers that are simulated by CLM5 (roughly corresponding to 0–50 cm depth). The *met* files also include daily GPP, air temperature, and N deposition that are simulated by CLM5 and required to run CASA-CNP. Additional input data needed to run the biogeochemical model testbed include soil texture (sand and clay fraction) and dominant plant functional type (PFT) distributions, which are also taken from CLM5 surface data sets.

Initial conditions in the biogeochemical model testbed were generated by spinning up vegetation and soil C pools by cycling over simulation years from (1901–1920) until steady-state conditions were reached. We did this in four model experiments: for C-only and CN versions of both MIMICS and CASA that were coupled to the CASA vegetation model. GPP was identical in all four of these simulations. Net primary production (NPP) and litterfall fluxes were identical for both the MIMICS-C and CASA-C simulations, reflecting autotrophic respiration parameterizations in the CASA-C vegetation model. Nitrogen limitation of NPP, however, reduced litterfall fluxes in the MIMICS-CN and CASA-CN experiments—reflecting differences in the N limitation experienced by plants, given the feedback from different soil biogeochemical models. Specifically, when daily inorganic N pools are less than 1g N m^{-2}, the CASA vegetation model increases autotrophic respiration fluxes, thereby reducing NPP. Differences in steady-state initial conditions are described in Section 3.1. Subsequently we ran transient simulations over the historical period from 1901 to 2014 for each of our four model experiments, with results described in Section 3.2. We did not run the biogeochemical model testbed with transient land use or land cover change.

2.2. MIMICS-CN

In this section we describe highlights of this global-scale implementation of CN biogeochemistry in MIMICS and provide relevant information about underlying assumptions and approaches taken in the MIMICS and CASA soil models. Notable features of MIMICS include the representation of metabolic and structural litter pools (LIT_m and LIT_s), explicit representation of fast and slow growing microbial functional groups (MIC_r and MIC_K), and the representation of physicochemically protected, chemically protected, and available SOM pools (SOM_p, SOM_c, and SOM_a; Figure 1). A similar wiring diagram and description for the CASA-CN model is included in Figure S1 in Supporting Information S1.

The basic structure of MIMICS-CN is described in Kyker-Snowman et al. (2020) and Eastman et al. (2023) and has not been changed from previous versions of MIMICS-C (Wieder, Cleveland, et al., 2015). As in our previous work (Wieder et al., 2018, 2019), MIMICS-CN uses temperature-sensitive reverse Michaelis-Menten kinetics to describe microbial community catabolic capacity (blue lines, Figure 1), which determine rates of litter and SOM decomposition that are modified by soil liquid water availability. MIMICS-CN also represents microbial growth efficiency that controls the fate of C and N fluxes in soils through microbial carbon use efficiency, nitrogen use efficiency, and microbial turnover (CUE, NUE, and τ, respectively; green lines, Figure 1), which are a function of substrate quality and microbial functional groups. Microbial necromass fluxes from each microbial functional group are allocated to different SOM pools, which vary as a function of soil clay content and litter quality (orange lines, Figure 1). Litter quality is inversely related to the allocation of microbial residues (f_c) that enter the chemically protected (SOM_c) pool. Soil clay content controls allocation to and turnover (f_p and D, respectively) of the physicochemically protected (SOM_p) pool in MIMICS.

Litterfall inputs (I) in MIMICS and CASA are partitioned into litter pools based on chemical quality, specifically the weighted average lignin:N ratio of all litter inputs determines the fraction of metabolic litter (f_{MET}) as in Parton et al. (1987) and applied by Wieder et al. (2014). One notable difference, however, is that fluxes from the
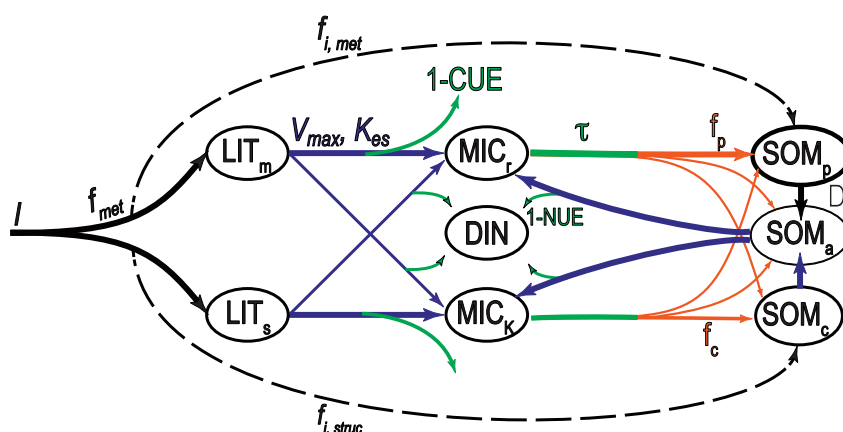
Figure 1. Pools of litter, microbial biomass, and soil organic matter (LIT, MIC, and SOM, respectively) that are represented in the MIcrobial-MIneral Carbon Stabilization-carbon-nitrogen model. Microbial catabolic potential (blue lines) varies with daily soil temperature and soil moisture and drives the decomposition of litter and SOM. Microbial growth rates (green lines) are determined by carbon use efficiency, nitrogen use efficiency, and turnover (CUE, NUE, and τ). CUE and NUE contribute to heterotrophic respiration and nitrogen mineralization fluxes, which occur for all fluxes into microbial biomass pools (but are not shown for clarity). Microbial necromass is partitioned into SOM pools as a function of soil clay content and litter quality (orange lines).

decay of coarse woody debris are transferred into structural litter pools in MIMICS, thus the lignin:N ratio associated with this flux is also included in the calculation of f_{MET}. By contrast, fluxes of coarse woody debris in CASA are transferred directly to SOM pools and, therefore, not included in the CASA calculation of f_{MET}. In MIMICS-CN we hold the stoichiometry of the metabolic litter inputs (and therefore the LIT_m pool) constant, assuming that this relatively labile litter flux has a high chemical quality (C:N = 15). Thus, the C:N of structural litter inputs (and the LIT_s pool) varies to conserve total N inputs from litterfall (Kyker-Snowman et al., 2020). A fraction of litter inputs bypasses the litter, and therefore microbial biomass pools, in MIMICS (f_i, Figure 1). The current parameterization of the model assumes a larger fraction of low quality, structural litter inputs are passed directly to the chemically protected SOM pool, which we think of as being analogous to a particulate organic matter (POM) pool (POM; $f_{i,\text{struc}} = 0.3$, or 30% of structural litter inputs). By contrast, relatively little metabolic litter directly contributes to the formation of physicochemically protected SOM, which we consider to be more like a mineral associated organic matter pool (MAOM; $f_{i,\text{met}} = 0.005$, or 0.5% of metabolic litter inputs). This change was made with the representation of N biogeochemistry in MIMICS-CN for site-level simulations by Kyker-Snowman et al. (2020) to increase the C:N ratio of bulk SOM pools, and also applied for global scale MIMICS-C and MIMICS-CN runs presented here. Lower input rates and turnover times to SOM_p pools were also implemented in the parameterization of MIMICS-CN presented here to achieve longer turnover times of this MAOM-like pool (Pierson et al., 2022; Wieder et al., 2019; H. Zhang et al., 2020).

The microbial functional groups represented in MIMICS are intended to represent functional trait tradeoffs between microbial growth rates (blue lines in Figure 1) and microbial growth efficiency and turnover (green lines in Figure 1) (Schimel & Schaeffer, 2012; Wieder et al., 2014). The model parameters reflect assumptions that a fast-growing microbial functional group (MIC_r) has a greater affinity for organic matter substrates with higher chemical quality (LIT_m) but has a lower CUE than a slower growing microbial functional group (MIC_K), which has a greater affinity for low chemical quality substrates (LIT_s) (Wieder et al., 2018).

Microbial stoichiometry in MIMICS-CN builds on this functional trait framework. We assumed that the higher catabolic potential (V_{max}) of MIC_r communities requires more nitrogen, resulting in lower microbial biomass C:N ratios, compared to slower growing copiotrophs. Kyker-Snowman et al. (2020) assign fixed C:N ratios for MIC_r and MIC_K—6 and 10 respectively, which generally reflects the mean C:N stoichiometry of bacteria and fungi (Cleveland & Liptzin, 2007). Total microbial biomass stoichiometry, therefore, reflects the relative abundance of these functional groups. Preliminary results using this approach in the biogeochemical model testbed, however, produced relatively constrained estimates for ecosystem microbial C:N ratios, compared to results from cross-biome syntheses (Cleveland & Liptzin, 2007) and subsequent global extrapolations (Gao et al., 2022; Xu et al., 2013). Substrate quality, however, influences microbial community composition and stoichiometry (Fanin

et al., 2013, 2014; Nemergut et al., 2010). Thus, we developed a simple parameterization that modifies the target microbial biomass stoichiometry as a function of litter quality (Equation 1)

$$CN_{target} = CN_{base} \sqrt{(CN_{mod}/f_{MET})} \qquad (1)$$

where the target CN ratio is the product of the base C:N ratio for copiotrophs and oligotrophs (6 and 10, respectively) and an empirical function using a CN modifier term (0.4 for these simulations) and f_{MET} (from litterfall inputs, Figure 1). This parameterization allows for somewhat greater spatial variability in microbial C:N ratios and is applied in the results presented here. Accordingly, the emergent microbial biomass stoichiometry that is simulated by MIMICS still reflects the relative abundance of microbial functional groups, but also the influences of litter quality.

Heterotrophic respiration fluxes in MIMICS are determined by the fluxes of C entering microbial biomass pools and associated CUE (Figure 1). In MIMICS, CUE varies by microbial functional group (higher for MIC_K than MIC_r, with a particular substrate) and substrate quality (e.g., LIT_m has a higher CUE than LIT_s for a given microbial functional group) (see technical documentation will wieder & melanniehartman, 2023). We assume that "messy eating" results in a 85% NUE on fluxes entering microbial biomass pools, with the remaining 15% of decomposed organic N being transferred to the dissolved inorganic nitrogen pool (DIN; models in the testbed do not simulate individual pools of ammonium and nitrate).

After accounting for these C and N losses from donor pool fluxes (coming from LIT_m, LIT_s, or SOM_a), MIMICS-CN evaluates the stoichiometry of incoming fluxes to the receiver pools (going to MIC_r or MIC_K) and their target stoichiometry. If the C:N ratio of total fluxes into microbial biomass pools is lower than their respective target, then this excess N is mineralized into the DIN pools. Conversely, if the C:N ratio of inputs to microbial biomass pools is higher than their respective targets then overflow respiration occurs, with this excess C added to the heterotrophic respiration flux. With the current model parameterization, microbial functional groups in MIMICS-CN are not generally C limited, which is generally consistent with empirical measurements and theoretical understanding (Soong et al., 2020), so overflow respiration fluxes are very small. Thus, in MIMICS-CN decomposition of litter and SOM pools proceeds independent from the size of the inorganic N pool. This approach differs from assumptions in the CASA soil biogeochemical model, which downregulates heterotrophic activity if inorganic N pools are $<1gN\ m^{-2}$ (Y. P. Wang et al., 2010). Similar assumptions are made in other soil biogeochemical models that downregulate decomposition rates under nitrogen limitation (Bonan et al., 2013; Thomas et al., 2015).

2.3. Analyses

We inferred soil C turnover times as the ratio of total soil C stocks and NPP simulated by the models at each grid cell at initialization (1901–1920 mean) (Koven et al., 2017). To compare inferred soil C turnover times between CN and C-only versions of both soil biogeochemical models we calculated response ratios, which were calculated as the natural log of the quotient of results from the CN and C-only versions of MIMICS and CASA; thus, response ratios of 0 signify that the CN and C-only versions of the model are identical. We assessed N limitation as the difference of NPP from CN and C-only simulations, such that more negative values reflect greater N limitation. We calculated net ecosystem production (NEP) as the difference of GPP and ecosystem respiration fluxes; thus, positive values of NEP values reflect net land C uptake. By definition, NEP is zero under steady-state, initial conditions.

We compared the latitudinal distribution and global sums for soil biogeochemical states and fluxes that were simulated by MIMICS and CASA with globally gridded estimates from database products. Specifically, we included total soil C stocks for 0–1 m depth from the Harmonized World Soils Database, version 1.2 (HWSD; FAO et al., 2012) that was regridded to a nominal 1° resolution (Wieder et al., 2014), Soil Grids, version 2.0 (Poggio et al., 2021; 500 m resolution was also regridded to a nominal 1° resolution), and the Northern Circumpolar Soil Carbon Database (NCSCD; Hugelius et al., 2013). We also compared microbial C and microbial C:N estimates from Xu et al. (2013); (see also Xu et al., 2014) and Serna-Chavez et al. (2013), heterotrophic respiration fluxes derived by Hashimoto et al. (2015), and soil C:N derived from the ratio of organic C and total N (0–1 m depth) from the Global Soil Data set for use in Earth System Models (GSDE; Shangguan

Table 1
Summary of Annual Fluxes and States Simulated by MIcrobial-MIneral Carbon Stabilization (MIMICS) and Carnegie-Ames-Stanford Approach (CASA) Models With Carbon-Nitrogen (CN) and C Biogeochemistry at Initialization

	MIMICS-CN	MIMICS-C	CASA-CN	CASA-C
GPP (Pg C yr^{-1})	106	106	106	106
NPP (Pg C yr^{-1})	38.2	42.0	38.9	42.0
HR (Pg C yr^{-1})	38.2	42.0	38.9	42.0
Total soil C (Pg C)	1,516	1,582	887	997
Total vegetation C (Pg C)	287	333	298	333
Microbial biomass (Pg C)	13.4	14.8	–	–
Relative microbial biomass C (%)	0.88	0.92	–	–
Net N mineralization (Tg N yr^{-1})	876	–	888	–
Total soil C:N	11.8	–	18.5	–
Microbial C:N	6.8	–	–	–

Note. Values represent globally integrated means of annual data simulated from 1901 to 1920. By definition, soil heterotrophic respiration fluxes (HR) are equal to net primary production (NPP) at initialization. Total soil C includes all litter, microbial biomass, and soil carbon pools simulated by the models. Relative microbial biomass is the fraction of the total soil C pool composed of microbial biomass and is shown as the global mean across all vegetated grid cells. Similarly, total soil C: N and microbial biomass C:N reflect global means for these quantities.

et al., 2014). We note that we are comparing steady state model results, intended to represent conditions at the start of the 20th century (1901–1920 mean state), with observations that are intended to be more representative of contemporary conditions. For slow turnover pools like bulk SOM, the latitudinal patterns presented here are unlikely to have appreciably changed over the historical period, but we acknowledge that microbial biomass and heterotrophic respiration are likely changing more rapidly.

3. Results

3.1. Initial Conditions

For initialization, all simulations received identical fluxes of GPP (106 Pg C yr^{-1}, global mean 1901–1920; Table 1). Lower NPP fluxes in MIMICS-CN and CASA-CN simulations reflect N limitation on plant growth, relative to the MIMICS-C and CASA-C simulations. MIMICS-CN simulated greater N-limitation in boreal forests (Figure S2 in Supporting Information S1) and had slightly lower NPP globally than results from CASA-CN (Table 1). With lower NPP and subsequent litterfall fluxes, steady-state soil C pools were also lower for CN versions of MIMICS and CASA than soil C stocks in each models' C-only counterpart. Initial global soil C stocks simulated by MIMICS totaled 1,516 and 1,582 Pg C (for CN and C-only simulations, respectively, including the sum of all litter, microbial biomass and soil C pools at 0–100 cm depth; Table 1). Initial soil C stocks simulated by CASA totaled 887 and 997 Pg C (again for CN and C-only simulations, respectively, Table 1).

Larger soil C pools in MIMICS-CN reflect longer inferred soil carbon turnover times than those simulated by CASA-CN (Figure 2a). Similar results were reported for the C-only versions of these models (Wieder et al., 2018) and reflect parametric and structural differences between the MIMICS and CASA soil biogeochemical models. The apparent banding in CASA simulations (Figure 2a) result from biome-specific soil C turnover times of slow and passive soil C pools, including notably rapid turnover times in agricultural soils (Y. P. Wang et al., 2010). MIMICS does not share this feature. Instead, longer turnover times simulated by MIMICS emerge from a common, global parameterization of the model.

The representation of CN biogeochemistry does not meaningfully alter soil C turnover times that are simulated by CASA-CN, but it does in MIMICS-CN (Figure 2b). In colder and drier biomes that are less productive, soil C turnover times increase in MIMICS-CN, relative to MIMICS-C. This occurs because N limitation of NPP reduces litterfall fluxes (Table 1). Microbial biomass pools in MIMICS, and other simper models, are proportional to litterfall inputs (Y. P. Wang et al., 2014). Microbial biomass also directly influences litter and soil C turnover times in models using Michaelis-Menten kinetics. Indeed, the response ratios of microbial biomass and inferred
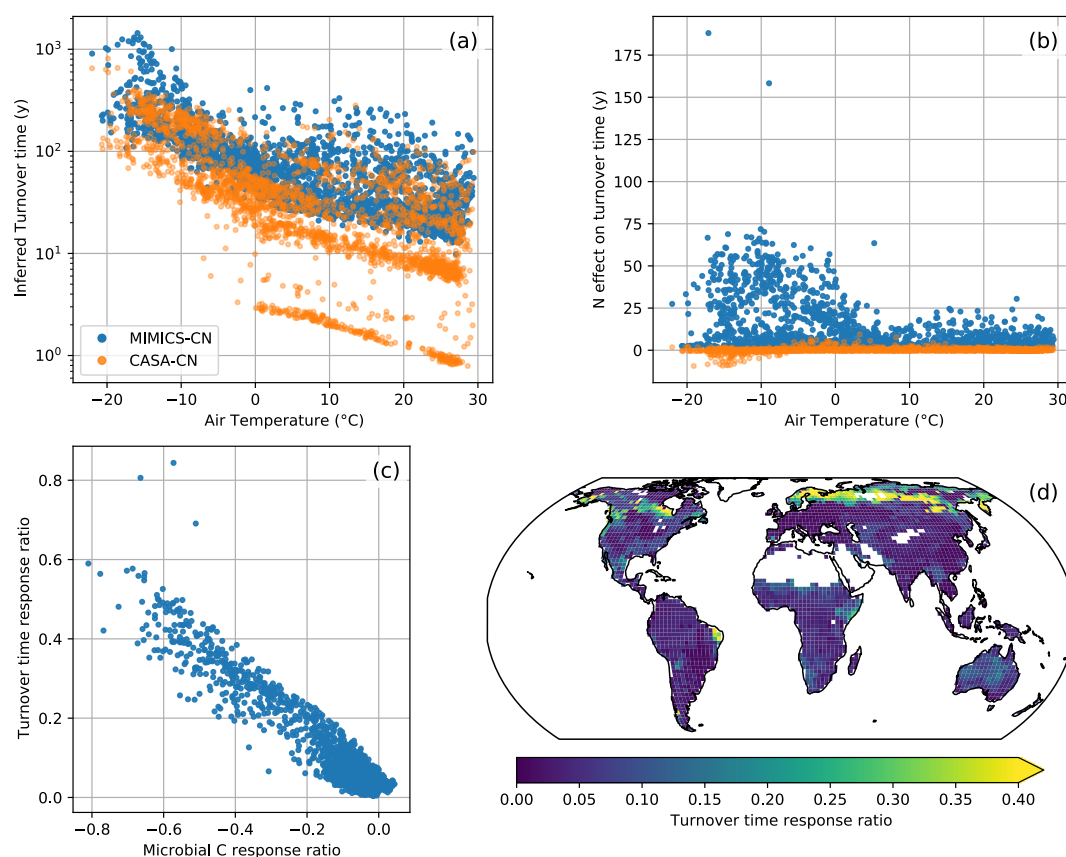
Figure 2. Inferred soil C turnover times as a function of mean annual air temperature (a) for all grid cells for the MIcrobial-MIneral Carbon Stabilization-carbon-nitrogen model (MIMICS-CN) and Carnegie-Ames-Stanford Approach (CASA-CN) simulations (blue and orange points, respectively) and (b) the difference in turnover times in CN configurations compared to the C-only versions of each model. Soil C turnover is calculated as the ratio of total soil C stocks and Net primary production (NPP) simulated by the models at initialization (1901–1920 mean). In MIMICS (c) the microbial biomass C response ratio in each grid cell is negatively correlated with the soil C turnover time response ratio. Response ratios are calculated at the natural log of the quotient of initial gridcell results from MIMICS-CN and MIMICS-C. The (d) soil C turnover time response ratio in MIMICS-CN is greatest in high-latitude ecosystems that also show stronger N limitation of NPP.

turnover times with MIMICS-CN show a strong, negative linear correlation (Figure 2c). Thus, longer soil C turnover times in MIMICS-CN resulted from N limitation of plant production that reduced microbial biomass pools and slowed turnover times, especially across high latitude ecosystems (Figure 2d).

All models show a latitudinal distributions of soil C stocks that agree reasonably well with observationally derived estimates (Figure 3a) and global soil C stocks to 1 m depth (1,690 Pg C from SoilGrids and 1,260 Pg C for the HWSD; Table 1). Microbial biomass carbon totals 13.1 and 14.8 Pg C globally in MIMICS-CN and MIMICS-C, respectively (Table 1). Global extrapolations from observational syntheses estimate microbial biomass C ranging from 14.6 to 23.2 Pg C (0–100 cm depth; Serna-Chavez et al., 2013; Xu et al., 2013). Both versions of MIMICS simulate larger microbial biomass pools in high latitude ecosystems, which fall within the large uncertainty from observationally upscaled estimates (Figure 3b). Globally, relative microbial biomass C (microbial C as a percent of total soil C stocks) is roughly 0.9% in MIMICS (Table 1), which is lower than observationally derived estimates of 1.2% from Serna-Chavez et al., 2013 (Figure 3c). Notably, MIMICS underestimates relative microbial biomass pools in temperate and tropical forests, compared with observationally derived estimates. Heterotrophic respiration fluxes that are simulated by MIMICS and CASA generally match latitudinal patterns from database estimates reported by Hashimoto et al. (2015; Figure 3d). At steady state, heterotrophic respiration fluxes are equal to NPP (Table 1). As such, this observational target provides more information about the quality of input data (here GPP derived from CLM and subsequent NPP calculated by the CASA vegetation model) than it does about heterotrophic respiration fluxes that are simulated by any of the soil biogeochemical models.
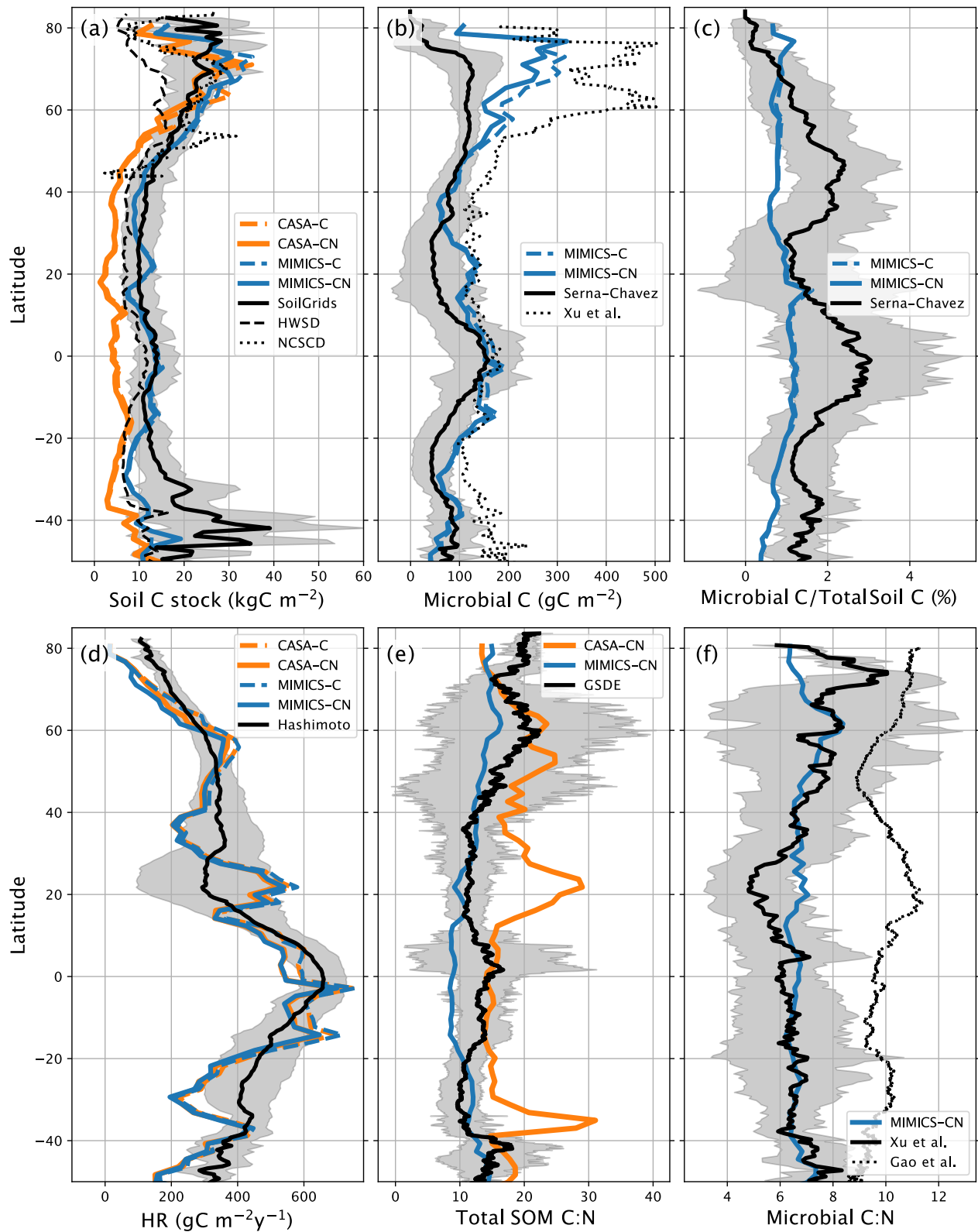
Figure 3.

Soil stoichiometry is prescribed for each PFT in CASA-CN, which produces high soil C:N ratios in semi-tropic, arid regions (Figure 3e). By contrast, the soil stoichiometry simulated by MIMICS-CN is an emergent property of the model. Both models demonstrate a relatively good match with global observations from Shangguan et al. (2014; Figure 3e), although MIMICS-CN underestimates soil C:N ratios across boreal forests and, to a lesser extent, in the tropics. MIMICS-CN predicts a latitudinal gradient in soil stoichiometry that largely reflects differences in microbial biomass and litterfall stoichiometry (Figure 4). Microbial biomass stoichiometry in MIMICS-CN is flexible within narrow ranges (see methods), but is also dependent on the relative abundance of microbial functional types (fast vs. slow). This approach produces global estimates of microbial C:N ratios of 6.8 (Table 1), which are close to observationally based upscaled estimates reported by Xu et al. (2013; global mean microbial C:N = 7.6), but lower than estimates from Gao et al. (2022; global mean microbial C:N = 10; Figure 3f).

The C:N ratio of SOM, microbial biomass, and litterfall fluxes that are simulated by MIMICS-CN are highest in boreal forests and lower in the tropics, especially in grassland and savanna regions (Figures 4a–4c). The stoichiometry of litter inputs as well as soil moisture control the relative abundance of fast versus slow microbial functional groups in the model. Accordingly, forests and arid regions tend to have a lower relative abundance of fast growing, copiotrophic microbes (Figure 4d). This largely reflects litter quality control over microbial community composition in the current parameterization of MIMICS-CN.

Soil texture and litter stoichiometry interact to determine the soil C:N ratios that are simulated by MIMICS-CN (Figure 5). For a given litter quality, higher clay fraction results in lower soil C:N ratios. For a given clay fraction, decreasing litter quality (higher litterfall C:N ratios) results in higher soil C:N ratios that are simulated by MIMICS. Both occur in MIMICS because increasing litter quality and clay content also increase the fraction of SOM that persists in the physicochemically protected SOM pool of the model (SOM_p). By contrast, CASA-CN parameterized soil stoichiometry based on PFT, resulting in higher soil C:N ratios than those simulated by MIMICS-CN (Figure 3e), but without evidence of the soil properties and litter quality effects on SOM stoichiometry (Figure 5b).

3.2. Transient Response

Global GPP simulated by CLM5 increased from 106 Pg C yr^{-1} at the start of the 20th century to 125 Pg C y^{-1} by the end of the historical period (here 2014). This led to an increase in NPP simulated by all the models, with the C-only models showing a slightly higher increase in NPP than the CN models (Table 2, Figure 6a, Figure S3 in Supporting Information S1). These increases in productivity and modest climate warming drove accelerated rates of heterotrophic respiration and net N mineralization in both models (Figures 6c and 6d). On balance, CASA simulations show accumulations of soil organic C and a more robust land C sink than MIMICS simulations, which indicate soil C losses and weaker (or neutral) land C uptake over the historical period (Figures 6e and 6f; Figure S3 in Supporting Information S1).

At initialization, MIMICS-CN showed slightly stronger N-limitation of NPP than CASA-CN (Table 1; Figure S2 in Supporting Information S1). Over the historical period, N limitation increased in both models, but more so in CASA-CN (Figure 6b). Greater vegetation C accumulation in MIMICS-CN, compared to CASA-CN (Table 2) was fueled by changes in soil biogeochemistry. Over the historical period, MIMICS-CN simulated larger increase in heterotrophic respiration and net N mineralization that resulted in soil C losses and a weak to neutral land C sink compared to CASA-CN, which accumulated soil C over this time and showed a stronger land C sink (Table 2; Figures 6c and 6f, Figure S3 in Supporting Information S1). Notably, MIMICS also simulated greater interannual variability in global C and N fluxes, compared to CASA simulations, despite receiving identical climate forcings (Figures 6b–6d).

Figure 3. Zonal mean plots for MIcrobial-MIneral Carbon Stabilization and Carnegie-Ames-Stanford Approach simulations (blue and orange lines, respectively) with coupled carbon-nitrogen (CN) biogeochemistry and C-only configuration (solid and dashed lines, respectively) and relevant observations (black lines with gray shading showing ±1 standard deviation of mean). Panels show (a) soil C stocks (kgC m^{-2}, 0–100 cm depth), (b) soil microbial biomass C stocks (gC m^{-2}, 0–100 cm depth), (c) relative microbial biomass C (microbial C as a percent of total soil C stocks) (d) soil heterotrophic respiration fluxes (gC m^{-2} yr^{-1}), (e) soil organic matter C:N ratio, and (f) microbial biomass C:N ratios. See methods for references of observations used in this analysis.
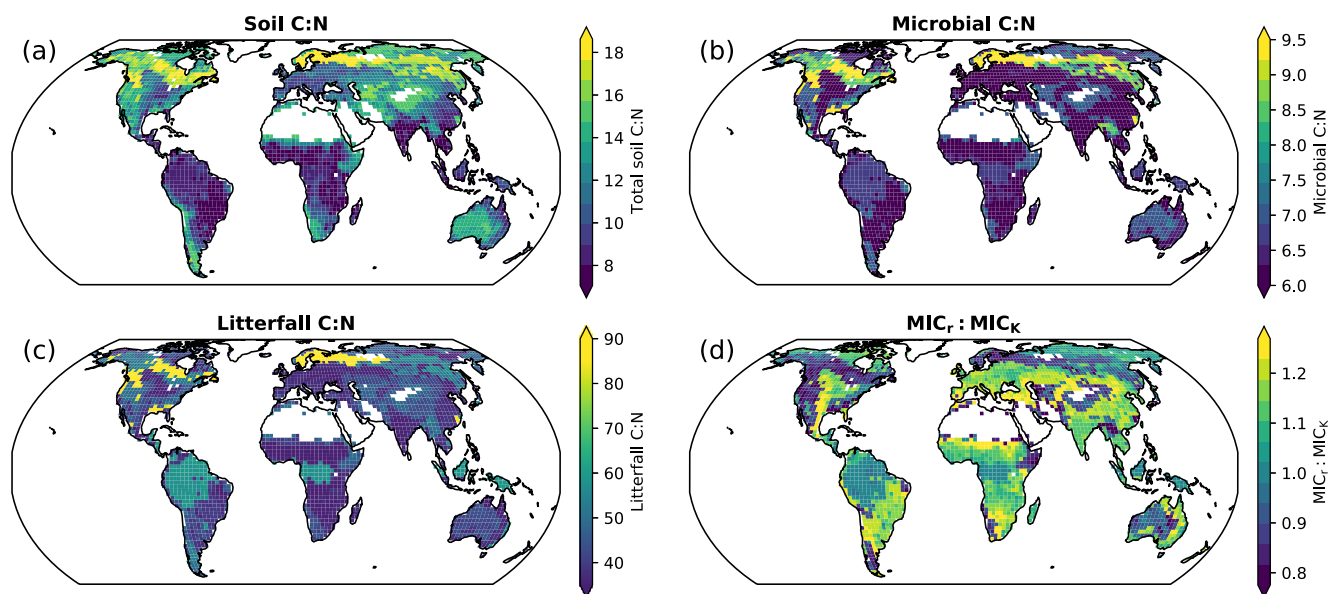
Figure 4. Spatial distribution of mean (a) soil C:N, (b) microbial biomass C:N, (c) litterfall C:N, and (d) the relative abundance of MIC$_r$:MIC$_K$ that were simulated by the MICrobial-MIneral Carbon Stabilization-carbon-nitrogen model at initialization (1901–1920).

A closer look at regional dynamics helps illuminate differences in MIMICS versus CASA simulations. Here we focus on the mean climatology of daily results simulated over a boreal forest region in Northern Europe (60–70°N and 0–100°E) at initialization (1901–1905 mean) and at the end of the historical period (2010–2014 mean). At steady state, MIMICS is more N limited than CASA (both globally and in this region; Figure S2 in Supporting Information S1, Figure 7). Over the historical period, however, MIMICS-CN becomes less N limited, largely because of temperature driven increases in SOM turnover and increases in N mineralization rates at high latitudes (Figure 7; Figure S3 in Supporting Information S1).

In our region of focus, mean NPP simulated during the model initialization period was 217 versus 265 gC m^{-2} yr^{-1} for MIMICS-CN and CASA-CN, respectively (Figure 7a; dashed lines). Low soil inorganic N concentrations simulated by both models caused this N limitation (Figures 7c and 7e). Collectively, these results illustrate differences in model sensitivities to cold soil temperatures that characterize the region. For most of the year, frozen soils more strongly limit microbial activity in MIMICS-CN, resulting in lower heterotrophic respiration and N mineralization fluxes in the boreal winter, spring, and fall, but higher rates during the warmer summer months (Figures 7b, 7d, 7f). Notably, annual heterotrophic respiration fluxes are equal to NPP fluxes that are simulated by both models at initialization; therefore, initial NEP equals zero for both models, but differences in the environmental sensitivities of MIMICS and CASA results in distinct seasonal climatologies of the timing of these fluxes during the year.

By the end of the historical period, differences in annual productivity that are simulated by the two models are reduced (Figure 7). Annual NPP totaled 291 versus 313 gC m^{-2} yr^{-1} in MIMICS-CN and CASA-CN, respectively; an increase of 34% and 18%, relative to their initial rates. Concurrently, in both models, warmer soil temperatures and higher productivity accelerate soil biogeochemical transformations. By the end of the historical period, annual heterotrophic rates increased by 30% and 14% in MIMICS-CN and CASA-CN, respectively, while net N mineralization rates increased by 39% and 20%, relative to their initial rates. These larger increases in N mineralization rates in MIMICS-CN reflect increases in SOM turnover as well as lower soil C:N ratio, compared to the CASA-CN simulations. In both models, this increases inorganic N availability, decreases the extent of N limitation, and fuels greater NPP. Although MIMICS-CN shows a stronger acceleration of NPP and HR fluxes over this domain, it still has dampened terrestrial C uptake (regional mean NEP = 9.1 and 10.0 gC m^{-2} yr^{-1} in MIMICS-CN and CASA-CN, respectively). By comparison NEP fluxes over this domain for C-only models show much larger spread (regional mean NEP = −12.0 and 10.9 gC m^{-2} yr^{-1} of MIMICS-C and CASA-C, respectively). Thus, inclusion of coupled CN biogeochemistry dampens the net carbon cycle response of both models
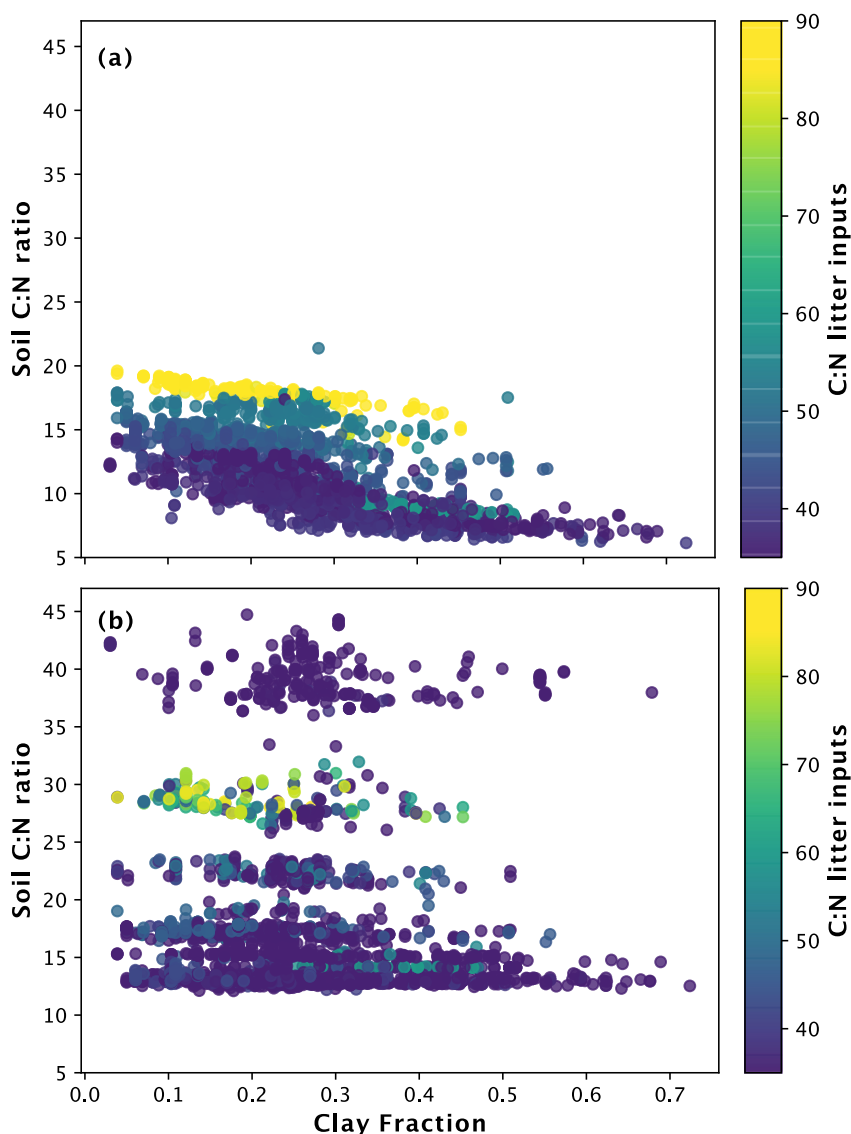
Figure 5. Soil texture and litter quality effects on soil C:N ratio that are simulated in (a) MIcrobial-MIneral Carbon Stabilization-carbon-nitrogen (MIMICS-CN) but not (b) Carnegie-Ames-Stanford Approach (CASA-CN). MIMICS-CN assumes that clay content and litterfall chemistry interact to determine bulk soil C:N ratios. By contrast, CASA-CN applies a biome-specific soil stoichiometric parameterization and does not reflect influences of soil texture or litter quality on soil C:N ratios. Coarse woody debris stoichiometry is considered in the litterfall C:N ratio in MIMICS-CN, but not in CASA-CN, which produces different litterfall stoichiometry estimates between the two models. The color bars used here match the one used in Figure 4c.

over the historical period, relative to the C-only models, a result that is also evident in our global results (Figure 6f).

4. Discussion

With common boundary conditions, the addition of coupled CN biogeochemistry to the MIMICS and CASA soil biogeochemical models produces global-scale results that are largely comparable with their respective C-only versions (Table 1). Steady-state soil C pools and turnover times that are simulated by MIMICS and CASA still show notable differences in their global sums and latitudinal distribution (Figures 2 and 3). Furthermore, simulation of coupled CN biogeochemistry dampens the C cycle response in transient simulations. Increasing N limitation in CASA-CN resulted in lower rates of vegetation C accrual over the historical period, compared with

Table 2
Summary of the Change in Annual Fluxes and States Simulated by MIcrobial-MIneral Carbon Stabilization (MIMICS) and Carnegie-Ames-Stanford Approach (CASA) Models With Carbon-Nitrogen (CN) and C Biogeochemistry at the End of the Historical Period

Δ in fluxes and states	MIMICS-CN	MIMICS-C	CASA-CN	CASA-C
GPP (Pg C yr^{-1})	15.5	15.5	15.5	15.5
NPP (Pg C yr^{-1})	5.5	5.6	5.5	5.6
HR (Pg C yr^{-1})	5.4	5.7	4.5	4.9
Total soil C (Pg C)	−14	−24	7	6
Total vegetation C (Pg C)	27	28	25	28
Microbial biomass (Pg C)	1.2	1.2	–	–
Relative microbial biomass C (%)	0.1	0.1	–	–
Net N mineralization (Tg N yr^{-1})	119	–	107	–
Total soil C:N	−0.07	–	−0.03	–
Microbial C:N	−0.03	–	–	–

Note. Values represent global sums and means of annual data from 1995 to 2014 subtracted by those calculated at initialization in Table 1.

the C-only simulations (Table 2, Figure 6); a finding that is consistent with previous modeling studies (Thornton et al., 2007; Y. P. Wang et al., 2010; Zaehle et al., 2010). By contrast, vegetation C accrual in MIMICS-CN nearly matched the MIMICS-C version of the model (Table 2). This occurred because higher rates of N mineralization were fueled by warming-induced accelerations of SOM decomposition over high latitude ecosystems during the historical period (Figures 6 and 7, Figure S2 in Supporting Information S1 see also Wieder et al., 2018). Thus, simulating CN biogeochemistry attenuated high latitude soil C losses that were simulated by MIMICS over the historical period, which increased cumulative NEP, relative to MIMICS-C.

Collectively, differences between MIMICS and CASA are larger than the effects of considering CN biogeochemistry in the respective models (see also Wieder et al., 2018; Wieder et al., 2019). Differences in model parameterizations and model structures are responsible for these findings, and should be explored in future research (Luo et al., 2016; Pierson et al., 2022; Shi et al., 2018; Y. P. Wang et al., 2021; H. Zhang et al., 2020). For example, more focused parameter calibration activities should reduce differences in steady-state soil C turnover time and stoichiometry between models (Figures 3 and 4). Subsequent transient responses to environmental perturbations, therefore, would more precisely identify biogeochemical outcomes that are related to differences in model structural assumptions. Although work presented here cannot definitively quantify the role of parametric versus model structural uncertainty in our results, we discuss some of the theoretical differences between explicit and implicit representations of microbial activity and their potential influence on emergent properties of the biogeochemical system.

The relatively subtle differences between C and CN versions CASA and MIMICS reflect the use of common boundary conditions in our simulations. Specifically, forcing the CASA vegetation model with the same GPP prevents soil N feedbacks from altering total ecosystem carbon inputs to each grid cell, thereby muting potential C cycle responses that are related to soil N biogeochemistry. More broadly, the similarity between C and CN versions of the models reflect the independent conceptualization and parameterization of respective C-only configurations, with subsequent addition of nitrogen biogeochemistry using stoichiometric constraints. This "carbon-first" development is common in terrestrial biogeochemical models (see Thomas et al., 2015), but it may reduce potential N feedbacks on the existing C-based framework of the models. In the approach taken in MIMICS, however, the simulated bulk soil C:N ratios are a more emergent property of the model, instead of static input parameters.

In the discussion that follows, we describe how our results highlight differences in the underlying assumptions of MIMICS and CASA. Subsequently, we discuss the advantages and drawbacks of using SOM C:N stoichiometry as an emergent property in soil biogeochemical models. Finally, we explore implications and future directions for applying microbial explicit structures to explore coupled C-nutrient dynamics in land models.

Figure 6. Change in global ecosystem fluxes and states simulated by MIcrobial-MIneral Carbon Stabilization and Carnegie-Ames-Stanford Approach (blue and orange lines, respectively) with C and CN biogeochemistry (dashed and solid lines, respectively). Panels show changes in global annual (a) net primary production (NPP), (b) nitrogen limitation of NPP (difference of CN and C simulations), (c) soil heterotrophic respiration, (d) net nitrogen mineralization (only for CN simulations), (e) total soil C, and (f) cumulative net ecosystem production. In all plots, the change is calculated as the difference between annual global means from the historical simulation and the initial (1901–1920) global mean.

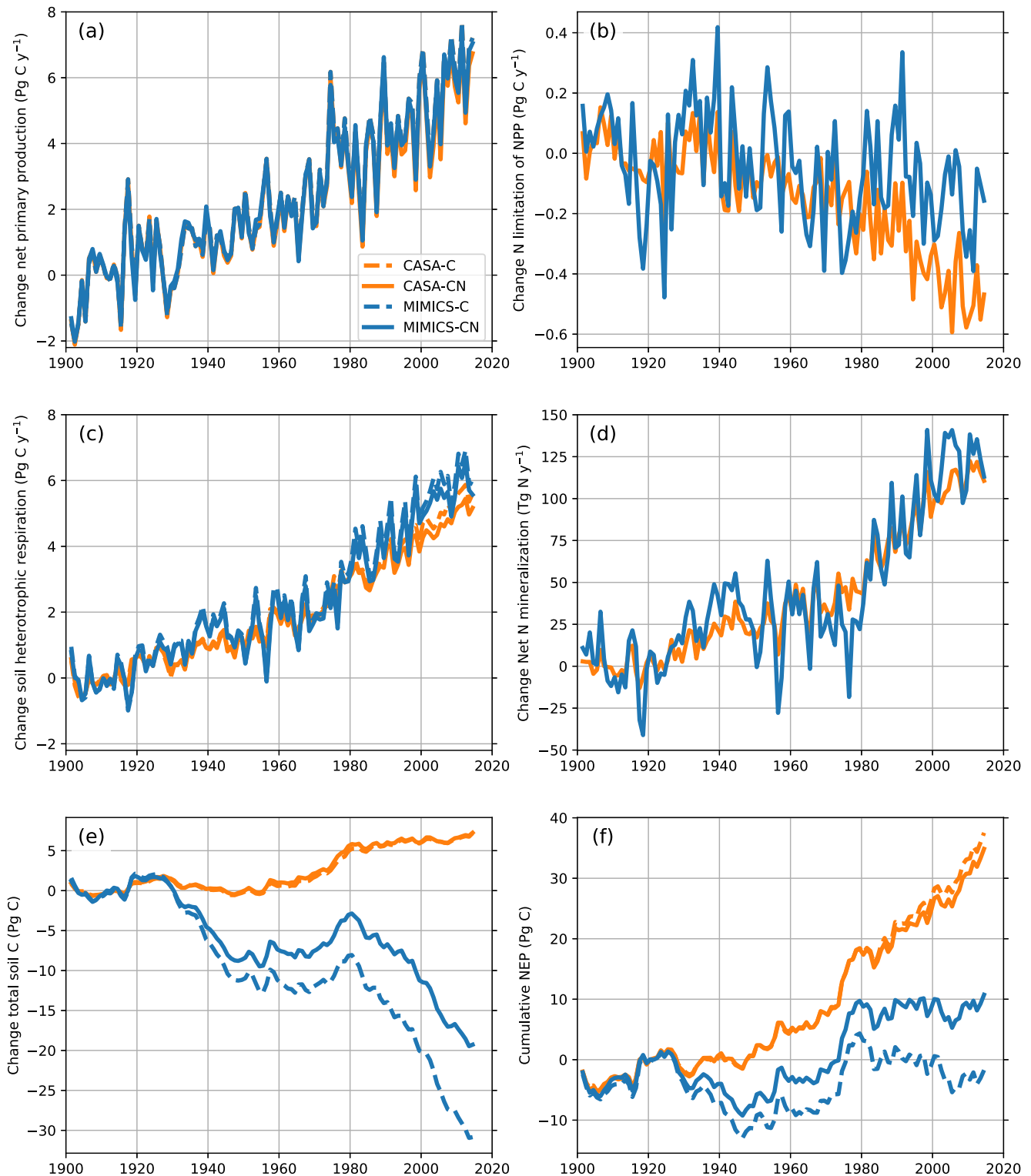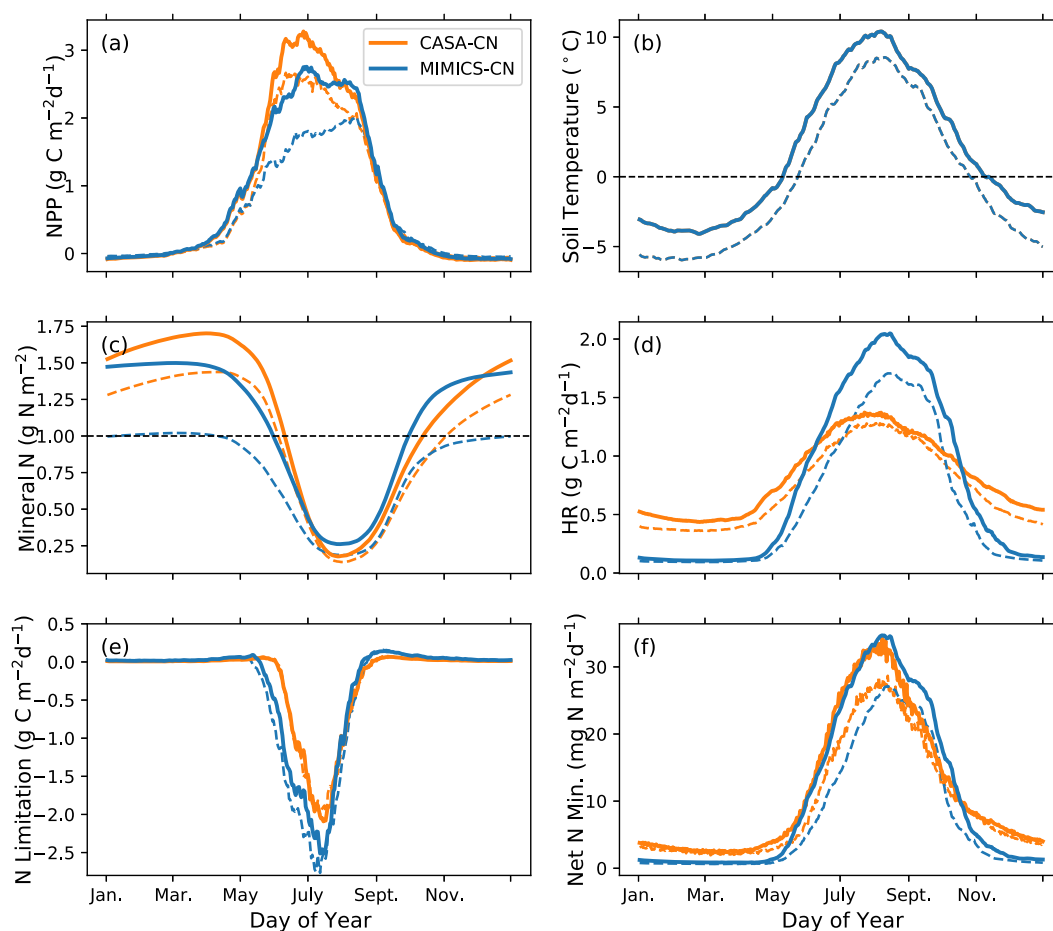**Figure 7.** Mean annual cycle of ecosystem fluxes and states simulated by MIcrobial-MIneral Carbon Stabilization and Carnegie-Ames-Stanford Approach (blue and orange lines, respectively) with coupled carbon-nitrogen biogeochemistry at the start (1901–1905; dashed line) end of the historical simulation (2010–2014; solid lines) over Northern Europe (60–70°N and 0–100°E). Panels show the annual cycle in the regionally averaged (a) net primary production (NPP), (b) soil temperature, (0–50 cm) (c) mineral N stocks, (d) heterotrophic respiration, (e) N limitation of NPP, and (f) net N mineralization rates.

4.1. Underlying Model Assumptions

The representation of CN biogeochemistry does not modify the steady-state turnover time of SOM pools that are represented by CASA, but it does in MIMICS (Figure 2). Models that implicitly represent microbial activity assume that the turnover time of SOM pools are determined by the inherent biochemical quality of substrates and modified by environmental scalars (Luo et al., 2016; Schimel, 2001). Accordingly, CASA simulations show no change in the inferred soil C turnover times with coupled CN biogeochemistry. By contrast, models that explicitly represent microbial activity assume that SOM turnover times are influenced by the size and activity of microbial biomass pools. This has important implications for both steady-state soil C pools, as well as seasonal dynamics of heterotrophic respiration (Basile et al., 2020; Jian et al., 2021) and N mineralization fluxes in microbially-explicit models like MIMICS (Figure 7).

Microbial biomass pools in MIMICS both build and decay SOM. The size of microbial biomass pools simulated in the model are proportional to litterfall C inputs (Wieder, Grandy, et al., 2015). Nitrogen limitation of NPP reduces litterfall, which also reduces microbial biomass pools that are simulated by MIMICS-CN (Table 1; Figure 3). Across all gridcells globally, the response of soil C turnover times in MIMICS-CN is negatively correlated with these changes in microbial biomass (Figure 2c). Thus, N limitation of NPP in the MIMICS-CN simulations reduces microbial biomass C and microbial catabolic potential to decompose SOM. This results in longer soil C turnover times, relative to the MIMICS-C simulations in MIMICS-CN. We see the largest effects of

N-limitation on NPP across high latitude ecosystems (Figure S2 in Supporting Information S1), where N effects on SOM turnover times are also most pronounced (Figure 2).

Explicitly representing microbial activity also influences temporal dynamics of soil biogeochemical fluxes that are simulated by MIMICS, and other microbial explicit models (Y. Huang et al., 2021). This is evident in the higher interannual variability of heterotrophic respiration and N mineralization fluxes that are simulated by MIMICS-CN (Figure 6). For example, regional biogeochemical fluxes that are simulated by MIMICS-CN show higher seasonal amplitude, a larger response to warming over the historical period, and a slight temporal lag in peak fluxes, relative to the CASA-CN simulations (Figure 7). Previous work found similar patterns with C-only versions of these models (Wieder et al., 2018) that have important implications on global estimates of terrestrial net ecosystem exchange of CO_2 with the atmosphere (Basile et al., 2020). The differences simulated by MIMICS and CASA, therefore, present opportunities for future studies to consider how changes in microbial physiology and phenology may impact the temporal dynamics of N mineralization rates and their feedback to ecosystem C and N fluxes under climate change scenarios.

The mathematical representation of nutrient limitation in land models continues to be challenging (Kou-Giesbrecht et al., 2023; Thomas et al., 2015). We recognize that CASA-CNP applies a relatively simplistic approach to plant N limitation by downregulating NPP and heterotrophic respiration rates when inorganic N pools are small (<1g N m^{-2}; Y. P. Wang et al., 2010). Similar assumptions are made by other microbial implicit soil biogeochemical models, which calculate potential rates of soil biogeochemical fluxes that are downregulated by nutrient availability (Lawrence et al., 2019; Yang et al., 2019; Zhu et al., 2019). By contrast, potential rates of litter and SOM decomposition are not downregulated by inorganic N availability in MIMICS-CN (Kyker-Snowman et al., 2020). Instead, if N availability is inadequate to meet microbial stoichiometric demands, then microbes reduce their effective CUE through overflow respiration fluxes that essentially burn off the excess carbon being decomposed. Additionally, the target stoichiometry of microbial communities varies as a function of litter quality in MIMICS-CN. Thus, the relative abundance of microbial functional groups shifts as a function of litter quality, but so too do their target C:N ratios (Figure 4; Equation 1). Although this approach still simplifies the diversity of strategies different decomposers use to meet stoichiometric imbalances between microbial communities and their resources (Mooshammer et al., 2014; Zechmeister-Boltenstern et al., 2015), the assumptions made in MIMICS-CN are more in line with concepts of microbial trait theory than those in CASA-CN.

In MIMICS, the size of the microbial biomass pool moderates SOM turnover times, and therefore N mineralization rates (Figure 2c). Accordingly, the relative size of microbial biomass pools, as a fraction of total soil C stocks, is a useful, first-order benchmark by which to evaluate microbial explicit models (Fierer et al., 2009; Serna-Chavez et al., 2013; Xu et al., 2013). The parameterization of MIMICS simulates larger relative microbial biomass pools in wetter ecosystems that support higher NPP (tropical and temperate forests) and smaller relative microbial biomass pools in drier, lower productivity regions (Figure 3c). This pattern aligns well with observational estimates synthesized by Serna-Chavez et al. (2013), who similarly found a correlation between moisture availability and relative microbial biomass C. We note that another synthesis (Xu et al., 2013) reports similar patterns, but also reports even higher relative microbial biomass C in deserts.

Beyond microbial biomass, cross-biome differences in microbial traits may ultimately be more valuable for informing and evaluating models that explicitly represent microbial activity. For example, plant trait variation across environmental gradients may be critical for representing biotic control (and variation) in terrestrial energy, water, and biogeochemical fluxes (Butler et al., 2017; Díaz et al., 2022). Similar information about environmental controls over soil microbial traits will be critical to further developing models that explicitly represent microbial activity. For example, cross-system syntheses suggest that the microbial strategies and biogeochemical function in arid systems may be distinct from more mesic environments (Fierer et al., 2012). Historical climate legacies may influence the physiological response of microbial communities to environmental change (Bradford et al., 2021; Evans & Wallenstein, 2014; Hawkes et al., 2020; Polussa et al., 2021). Finally, the phenology of microbial activity may lead to distinct seasonal shifts in microbial community composition (Lipson & Schmidt, 2004). In summary, mounting evidence suggests that microbial physiological traits show ecologically important variability over space and time, but they remain coarsely represented in the global parameterization of MIMICS-CN presented here. Thus, we see opportunities to further refine the model structure and parameterizations to improve the representation of microbial community composition and activity.

4.2. Stoichiometry as an Emergent Property

The stoichiometry of SOM in MIMICS-CN is an emergent property of the model, presenting opportunities to investigate model assumptions that produce variations in microbial biomass and SOM stoichiometry across climate, ecosystem, and edaphic gradients. In MIMICS-CN we assume that the higher catabolic capacity of fast growing copiotrophic microbial communities require more N and, therefore, these communities have a lower microbial biomass C:N ratio than slower growing oligotrophic communities. We also assume that the chemical quality of litter inputs modifies microbial biomass C:N, similar to assumptions made about litter quality and SOM stoichiometry in CASA and the CENTURY model (Parton et al., 1993). This results in relatively constrained estimates of microbial biomass C:N by MIMICS-CN, consistent with findings from observational syntheses (Cleveland & Liptzin, 2007; Xu et al., 2013). The spatial variation in microbial stoichiometry that is simulated by MIMICS is consistent with observationally derived extrapolations across latitudes (Figure 3f; Gao et al., 2022; Xu et al., 2013) and largely reflects differences in the relative abundance of fast and slow growing microbes and the chemical quality of litter inputs (Figures 4 and 5). Still, real ecosystems have larger variation in microbial stoichiometry than the MIMICS-CN simulations presented here (Kyker-Snowman et al., 2020), presenting opportunities to deepen understanding of the ecological factors that may mediate microbial community stoichiometry within and among ecosystems.

In MIMICS-CN we not only assume that microbial biomass pools determine rates of decomposition, but also the formation of persistent SOM (orange lines, Figure 1). Accordingly, the stoichiometry of SOM pools shows a strong microbial signature, in line with current understanding of SOM formation (Figure 4; Kyker-Snowman et al., 2020; Whalen et al., 2022). This results in somewhat narrower latitudinal gradients and spatial variation in SOM C:N than observationally derived estimates (Figure 3e). Collectively, however, MIMICS-CN makes clear assumptions that litter quality and soil texture are dominant controls over bulk soil C:N ratios that are simulated across ecosystems (Figure 5). Bulk soil C:N values more broadly reflect the relative abundance of physically versus chemically protected SOM, as expected theoretically and shown in observational data (Buchkowski et al., 2019; Cotrufo et al., 2019). For example, we assume clay-rich soils have a higher proportion of total SOM stocks in physicochemically protected (MAOM-like) pools (Grandy & Neff, 2008; Wieder et al., 2014). In MIMICS-CN the SOM_p pool has a low C:N ratio that reflects the dominant role of microbial residues in forming this persistent pool of SOM that has long turnover times. By contrast, in sandier soils MIMICS-CN assumes a higher proportion of total SOM stocks are in chemically protected (POM-like) pools. The SOM_c pool has a higher C:N ratio that reflects greater contributions of plant residues. Relative to MIMICS-C, the parameterization used in MIMICS-CN assumes that a greater fraction of structural litter inputs bypass the microbial filter to form SOM_c, which is similar to a POM pool (see also Kyker-Snowman et al., 2020). This modification was needed to increase the total soil C:N that is simulated in MIMICS-CN, although we also recognize that the current parameterization may overestimate the size of the SOM_c pool globally, and especially at high latitudes (Georgiou et al., 2024; Wieder et al., 2019).

Potential underestimation in bulk soil C:N ratios that are simulated by MIMICS-CN also underscore challenges in understanding plant versus microbial contributions to SOM formation (Simpson et al., 2007; Whalen et al., 2022). This is especially true for SOM that is protected by minerals and aggregates, which tend to have longer turnover times. In MIMICS-CN, we assume that plant-derived biomolecules have a higher C:N ratio than those that are microbial-derived (Cleveland & Liptzin, 2007; Mooshammer et al., 2014), reflecting stoichiometric differences that may be helpful in evaluating the underlying assumptions in the model. Notably, recent work finds that plant-derived biomolecules are abundant within protected SOM, especially in forested ecosystems (Angst et al., 2021). Elsewhere, Heckman et al. (2023) found that MAOM from humid, forest soils tends to have higher C:N ratios that is less decomposed than MAOM from drier, grassland ecosystems. Additionally, exo-enzyme transformation of plant inputs, as opposed to microbial turnover, may increase OM contribution to MAOM with a more plant-like signature (Liang et al., 2017). Collectively, these findings underscore broader uncertainties in quantifying plant versus microbial contributions to SOM formation (Whalen et al., 2022), but they also suggest that the current parameterization of MIMICS-CN may overemphasize the importance of microbial biomass contributions to protected SOM, which may also explain the underestimation of bulk soil C:N ratios in our results.

In contrast to the emergent stoichiometry that reflects underlying assumptions made in MIMICS-CN, spatial variation in soil stoichiometry simulated by CASA-CN is less nuanced (Figure 5). In models that implicitly represent microbial activity (including CASA-CN) receiver pool stoichiometry is parameterized, either with a

fixed value for particular pools (e.g.,; lower C:N targets for the passive pool, ∼11–12, compared to the slow pool, C:N ∼12–20), that may also vary PFT (Koven et al., 2013; Y. P. Wang et al., 2010). This PFT-specific parameterization of SOM stoichiometry results in latitudinal gradients of soil C:N ratios simulated by CASA-CN (Figure 3e). Stoichiometric flexibility is achieved through a linear function between soil C:N ratios and soil mineral N availability, which reduces receiver pool demand for N when mineral N availability is low and buffers soil C turnover from becoming limited by inorganic N availability (Bonan et al., 2013; Meyerholt & Zaehle, 2015; Parton et al., 1993; Y. P. Wang et al., 2010). Warmer sites have higher N mineralization rates and (slightly) lower soil C:N ratios, but in general soil stoichiometry simulated by CASA-CN largely reflects the PFT-specific parameterization applied in the model. While this parameterization of stoichiometric flexibility reflects foundational understanding of N mineralization, it has recently been suggested that N mineralization may be limited by desorption of N-rich MAOM, which is not well represented in MIMICS-CN or CASA-CN (Jilling et al., 2018, 2021; Schimel et al., 2004).

4.3. Implications and Future Directions

Our results illustrate the feasibility of conducting global scale simulations with a microbial explicit soil biogeochemical model under climate change scenarios. In both MIMICS and CASA simulations the inclusion of CN biogeochemistry attenuates or dampens the magnitude of ecosystem C responses to climate change over the historical period. The explicit representation of microbial activity in MIMICS-CN modifies steady-state and transient behavior of the model, relative to MIMICS-C. For example, by reducing litterfall and microbial biomass C, representing CN biogeochemistry increases the steady-state turnover time of SOM that is simulated by MIMICS-CN. Moreover, whereas nutrient limitation typically slows down decomposition of SOM pools that are simulated by microbial implicit models, MIMICS does not share this assumption, allowing for overflow respiration of excess C instead. However, concentration alone may not predict nutrient availability and future model development could include plant and microbial competition and other mechanisms underlying nutrient availability.

Beyond this direct consideration of nutrient limitation, shifts in plant and microbial resource allocation in response to global change drivers are important to consider, but only rudimentarily represented in the biogeochemical model testbed. For example, elevated CO_2 and N enrichment can alter plant belowground allocation, fine root stoichiometry, and microbial community composition (Drigo et al., 2010; Jia et al., 2023; Knops et al., 2007). Recent evidence shows that belowground C inputs are more efficiently stabilized on mineral surfaces and in aggregates (Austin et al., 2017; Sokol & Bradford, 2018). At the same time, root exudates and organic acids can prime decomposition of existing SOM and even destabilize MAOM to accelerate heterotrophic respiration and ecosystem C losses (Keiluweit et al., 2015; van Groenigen et al., 2014). Thus, the net effects of changing belowground C inputs on the long-term persistence of SOM, N mineralization rates, and feedbacks to NPP ultimately influence the magnitude and direction of net terrestrial exchange of CO_2 with the atmosphere. Current assumptions made in the biogeochemical model testbed do not easily allow consideration of these dynamics. Future research will refine understanding of plant-soil feedbacks and apply these insights in an ensemble of models that represent coupled CN biogeochemistry.

Finally, by allowing SOM stoichiometry to be an emergent property of the model, we see opportunities to use MIMICS-CN to deepen understanding of plant versus microbial sources of persistent SOM (Whalen et al., 2022). MIMICS-CN could also be altered to test alternative controls of N mineralization, such as desorption from the N-rich MAOM pool (Jilling et al., 2018). Further, soil C:N is a valuable metric for understanding soil C storage, N availability, and the N requirement of C storage (Averill, 2014; Cotrufo et al., 2019). The emergent stoichiometry in MIMICS-CN will allow for exploration of potential sensitivities of soil C:N to environmental change across gradients in soil properties, ecosystems, and climate, which have been inconsistently documented in observational studies (Keller et al., 2022; Rocci et al., 2022; Yue et al., 2017). Moreover, theory and measurements point to organisms' ability to optimize metabolic carbon use efficiency to overcome elemental imbalances between substrates and organismal stoichiometry (Manzoni et al., 2017). Future work should evaluate if the parameterization of MIMICS-CN can replicate these observed patterns across terrestrial ecosystems. Overall, applying coupled CN biogeochemistry in a microbially explicit model at the global scale for the first time allowed us to evaluate the effect of including microbes explicitly and also N, rather than solely C, which provided insight for model parameterizations but also future avenues of exploration.

Conflict of Interest

The authors declare no conflicts of interest relevant to this study.

Data Availability Statement

Model code and scripts used to generate figures are available from will wieder and melanniehartman (2023). Data including meteorological drivers and testbed output are available from Wieder and Hartman (2023).

References

Angst, G., Mueller, K. E., Nierop, K. G. J., & Simpson, M. J. (2021). Plant- or microbial-derived? A review on the molecular composition of stabilized soil organic matter. *Soil Biology and Biochemistry*, *156*, 108189. https://doi.org/10.1016/j.soilbio.2021.108189

Austin, E. E., Wickings, K., McDaniel, M. D., Robertson, G. P., & Grandy, A. S. (2017). Cover crop root contributions to soil carbon in a no-till corn bioenergy cropping system. *GCB Bioenergy*, *9*(7), 1252–1263. https://doi.org/10.1111/gcbb.12428

Averill, C. (2014). Divergence in plant and microbial allocation strategies explains continental patterns in microbial allocation and biogeochemical fluxes. *Ecology Letters*, *17*(10), 1202–1210. https://doi.org/10.1111/ele.12324

Averill, C., Turner, B. L., & Finzi, A. C. (2014). Mycorrhiza-mediated competition between plants and decomposers drives soil carbon storage. *Nature*, *505*(7484), 543–545. https://doi.org/10.1038/nature12901

Basile, S. J., Lin, X., Wieder, W. R., Hartman, M. D., & Keppel-Aleks, G. (2020). Leveraging the signature of heterotrophic respiration on atmospheric CO_2 for model benchmarking. *Biogeosciences*, *17*(5), 1293–1308. https://doi.org/10.5194/bg-17-1293-2020

Bonan, G. B., Hartman, M. D., Parton, W. J., & Wieder, W. R. (2013). Evaluating litter decomposition in earth system models with long-term litterbag experiments: An example using the community land model version 4 (CLM4). *Global Change Biology*, *19*(3), 957–974. https://doi.org/10.1111/gcb.12031

Bonan, G. B., Lombardozzi, D. L., Wieder, W. R., Oleson, K. W., Lawrence, D. M., Hoffman, F. M., & Collier, N. (2019). Model structure and climate data uncertainty in historical simulations of the terrestrial carbon cycle (1850–2014). *Global Biogeochemical Cycles*, *33*(10), 1310–1326. https://doi.org/10.1029/2019gb006175

Bradford, M. A., Wood, S. A., Addicott, E. T., Fenichel, E. P., Fields, N., González-Rivero, J., et al. (2021). Quantifying microbial control of soil organic matter dynamics at macrosystem scales. *Biogeochemistry*, *156*(1), 19–40. https://doi.org/10.1007/s10533-021-00789-5

Buchkowski, R. W., Shaw, A. N., Sihi, D., Smith, G. R., & Keiser, A. D. (2019). Constraining carbon and nutrient flows in soil with ecological stoichiometry. *Frontiers in Ecology and Evolution*, *7*, 13630. https://doi.org/10.3389/fevo.2019.00382

Butler, E. E., Datta, A., Flores-Moreno, H., Chen, M., Wythers, K. R., Fazayeli, F., et al. (2017). Mapping local and global variability in plant trait distributions. *Proceedings of the National Academy of Sciences USA*, *114*(51), E10937–E10946. https://doi.org/10.1073/pnas.1708984114

Cleveland, C. C., & Liptzin, D. (2007). C:N:P stoichiometry in soil: Is there a "Redfield ratio" for the microbial biomass? *Biogeochemistry*, *85*(3), 235–252. https://doi.org/10.1007/s10533-007-9132-0

Cotrufo, M. F., Ranalli, M. G., Haddix, M. L., Six, J., & Lugato, E. (2019). Soil carbon storage informed by particulate and mineral-associated organic matter. *Nature Geoscience*, *12*(12), 989–994. https://doi.org/10.1038/s41561-019-0484-6

Cotrufo, M. F., Wallenstein, M. D., Boot, C. M., Denef, K., & Paul, E. (2013). The microbial efficiency-matrix stabilization (MEMS) framework integrates plant litter decomposition with soil organic matter stabilization: Do labile plant inputs form stable soil organic matter? *Global Change Biology*, *19*(4), 988–995. https://doi.org/10.1111/gcb.12113

Díaz, S., Kattge, J., Cornelissen, J. H. C., Wright, I. J., Lavorel, S., Dray, S., et al. (2022). The global spectrum of plant form and function: Enhanced species-level trait dataset. *Scientific Data*, *9*(1), 755. https://doi.org/10.1038/s41597-022-01774-9

Drigo, B., Pijl, A. S., Duyts, H., Kielak, A. M., Gamper, H. A., Houtekamer, M. J., et al. (2010). Shifting carbon flow from roots into associated microbial communities in response to elevated atmospheric CO_2. *Proceedings of the National Academy of Sciences of the United States of America*, *107*(24), 10938–10942. https://doi.org/10.1073/pnas.0912421107

Dunne, J. P., Horowitz, L. W., Adcroft, A. J., Ginoux, P., Held, I. M., John, J. G., et al. (2020). The GFDL earth system model version 4.1 (GFDL-ESM 4.1): Overall coupled model description and simulation characteristics. *Journal of Advances in Modeling Earth Systems*, *12*(11), e2019MS002015. https://doi.org/10.1029/2019ms002015

Eastman, B. A., Wieder, W. R., Hartman, M. D., Brzostek, E. R., & Peterjohn, W. T. (2023). Can models adequately reflect how long-term nitrogen enrichment alters the forest soil carbon cycle? *Biogeosciences Discussions*, *2023*, 1–33. https://doi.org/10.5194/bg-2023-36

Elser, J. J., Bracken, M. E. S., Cleland, E. E., Gruner, D. S., Harpole, W. S., Hillebrand, H., et al. (2007). Global analysis of nitrogen and phosphorus limitation of primary producers in freshwater, marine and terrestrial ecosystems. *Ecology Letters*, *10*(12), 1135–1142. https://doi.org/10.1111/j.1461-0248.2007.01113.x

Evans, S. E., & Wallenstein, M. D. (2014). Climate change alters ecological strategies of soil bacteria. *Ecology Letters*, *17*(2), 155–164. https://doi.org/10.1111/ele.12206

Fanin, N., Fromin, N., Buatois, B., & Hattenschwiler, S. (2013). An experimental test of the hypothesis of non-homeostatic consumer stoichiometry in a plant litter-microbe system. *Ecology Letters*, *16*(6), 764–772. https://doi.org/10.1111/ele.12108

Fanin, N., Hättenschwiler, S., & Fromin, N. (2014). Litter fingerprint on microbial biomass, activity, and community structure in the underlying soil. *Plant and Soil*, *379*(1–2), 79–91. https://doi.org/10.1007/s11104-014-2051-7

FAO, IIASA, ISRIC, ISSCAS, & JRC. (2012). Harmonized World soil database (version 1.2) [Dataset]. *Rome, Italy and IIASA, Laxenburg, Austria*. https://www.fao.org/soils-portal/data-hub/soil-maps-and-databases/harmonized-world-soil-database-v12/en/

Fierer, N., Leff, J. W., Adams, B. J., Nielsen, U. N., Bates, S. T., Lauber, C. L., et al. (2012). Cross-biome metagenomic analyses of soil microbial communities and their functional attributes. *Proceedings of the National Academy of Sciences*, *109*(52), 21390–21395. https://doi.org/10.1073/pnas.1215210110

Fierer, N., Strickland, M. S., Liptzin, D., Bradford, M. A., & Cleveland, C. C. (2009). Global patterns in belowground communities. *Ecology Letters*, *12*(11), 1238–1249. https://doi.org/10.1111/j.1461-0248.2009.01360.x

Gao, D., Bai, E., Wang, S., Zong, S., Liu, Z., Fan, X., et al. (2022). Three-dimensional mapping of carbon, nitrogen, and phosphorus in soil microbial biomass and their stoichiometry at the global scale. *Global Change Biology*, *28*(22), 6728–6740. https://doi.org/10.1111/gcb.16374

Georgiou, K., Koven, C. D., Wieder, W. R., Hartman, M. D., Riley, W. J., Pett-Ridge, J., et al. (2024). Emergent temperature sensitivity of soil organic carbon driven by mineral associations. *Nature Geoscience*, *17*(3), 205–212. https://doi.org/10.1038/s41561-024-01384-7

Grandy, A. S., & Neff, J. C. (2008). Molecular C dynamics downstream: The biochemical decomposition sequence and its impact on soil organic matter structure and function. *Science of the Total Environment*, *404*(2–3), 297–307. https://doi.org/10.1016/j.scitotenv.2007.11.013

Hashimoto, S., Carvalhais, N., Ito, A., Migliavacca, M., Nishina, K., & Reichstein, M. (2015). Global spatiotemporal distribution of soil respiration modeled using a global database. *Biogeosciences*, *12*(13), 4121–4132. https://doi.org/10.5194/bg-12-4121-2015

Hawkes, C. V., Shinada, M., & Kivlin, S. N. (2020). Historical climate legacies on soil respiration persist despite extreme changes in rainfall. *Soil Biology and Biochemistry*, *143*, 107752. https://doi.org/10.1016/j.soilbio.2020.107752

Heckman, K. A., Possinger, A. R., Badgley, B. D., Bowman, M. M., Gallo, A. C., Hatten, J. A., et al. (2023). Moisture-driven divergence in mineral-associated soil carbon persistence. *Proceedings of the National Academy of Sciences*, *120*(7), e2210044120. https://doi.org/10.1073/pnas.2210044120

Huang, Y., Guenet, B., Ciais, P., Janssens, I. A., Soong, J. L., Wang, Y., et al. (2018). ORCHIMIC (v1.0), a microbe-mediated model for soil organic matter decomposition. *Geoscientific Model Development*, *11*(6), 2111–2138. https://doi.org/10.5194/gmd-11-2111-2018

Huang, Y., Guenet, B., Wang, Y. L., & Ciais, P. (2021). Global simulation and evaluation of soil organic matter and microbial carbon and nitrogen stocks using the microbial decomposition model ORCHIMIC v2.0. *Global Biogeochemical Cycles*, *35*(5), e2020GB006836. https://doi.org/10.1029/2020gb006836

Hugelius, G., Tarnocai, C., Broll, G., Canadell, J. G., Kuhry, P., & Swanson, D. K. (2013). The northern circumpolar soil carbon database: Spatially distributed datasets of soil coverage and soil carbon storage in the northern permafrost regions. *Earth System Science Data*, *5*(1), 3–13. https://doi.org/10.5194/essd-5-3-2013

Jia, W., Zheng, T., Zhao, Y., Deng, F., Yang, Y., Liang, C., et al. (2023). Nitrogen application influences the effect of bacteria on the belowground allocation of photosynthesized carbon under elevated CO_2. *Soil Biology and Biochemistry*, *180*, 109021. https://doi.org/10.1016/j.soilbio.2023.109021

Jian, J., Bond-Lamberty, B., Hao, D., Sulman, B. N., Patel, K. F., Zheng, J., et al. (2021). Leveraging observed soil heterotrophic respiration fluxes as a novel constraint on global-scale models. *Global Change Biology*, *27*(20), 5392–5403. https://doi.org/10.1111/gcb.15795

Jilling, A., Keiluweit, M., Contosta, A. R., Frey, S., Schimel, J., Schnecker, J., et al. (2018). Minerals in the rhizosphere: Overlooked mediators of soil nitrogen availability to plants and microbes. *Biogeochemistry*, *139*(2), 103–122. https://doi.org/10.1007/s10533-018-0459-5

Jilling, A., Keiluweit, M., Gutknecht, J. L. M., & Grandy, A. S. (2021). Priming mechanisms providing plants and microbes access to mineral-associated organic matter. *Soil Biology and Biochemistry*, *158*, 108265. https://doi.org/10.1016/j.soilbio.2021.108265

Keiluweit, M., Bougoure, J. J., Nico, P. S., Pett-Ridge, J., Weber, P. K., & Kleber, M. (2015). Mineral protection of soil carbon counteracted by root exudates. *Nature Climate Change*, *5*(6), 588–595. https://doi.org/10.1038/nclimate2580

Keller, A. B., Borer, E. T., Collins, S. L., DeLancey, L. C., Fay, P. A., Hofmockel, K. S., et al. (2022). Soil carbon stocks in temperate grasslands differ strongly across sites but are insensitive to decade-long fertilization. *Global Change Biology*, *28*(4), 1659–1677. https://doi.org/10.1111/gcb.15988

Knops, J. M. H., Naeem, S., & Reich, P. B. (2007). The impact of elevated CO_2, increased nitrogen availability and biodiversity on plant tissue quality and decomposition. *Global Change Biology*, *13*(9), 1960–1971. https://doi.org/10.1111/j.1365-2486.2007.01405.x

Kou-Giesbrecht, S., Arora, V. K., Seiler, C., Arneth, A., Falk, S., Jain, A. K., et al. (2023). Evaluating nitrogen cycling in terrestrial biosphere models: A disconnect between the carbon and nitrogen cycles. *Earth System Dynamics*, *14*(4), 767–795. https://doi.org/10.5194/esd-14-767-2023

Koven, C. D., Hugelius, G., Lawrence, D. M., & Wieder, W. R. (2017). Higher climatological temperature sensitivity of soil carbon in cold than warm climates. *Nature Climate Change*, *7*(11), 817–822. https://doi.org/10.1038/nclimate3421

Koven, C. D., Riley, W. J., Subin, Z. M., Tang, J. Y., Torn, M. S., Collins, W. D., et al. (2013). The effect of vertically-resolved soil biogeochemistry and alternate soil C and N models on C dynamics of CLM4. *Biogeosciences*, *10*(11), 7109–7131. https://doi.org/10.5194/bg-10-7109-2013

Kyker-Snowman, E., Wieder, W. R., Frey, S. D., & Grandy, A. S. (2020). Stoichiometrically coupled carbon and nitrogen cycling in the MIcrobial-MIneral Carbon Stabilization model version 1.0 (MIMICS-CN v1.0). *Geoscientific Model Development*, *13*(9), 4413–4434. https://doi.org/10.5194/gmd-13-4413-2020

Lawrence, D. M., Fisher, R. A., Koven, C. D., Oleson, K. W., Swenson, S. C., Bonan, G., et al. (2019). The community land model version 5: Description of new features, benchmarking, and impact of forcing uncertainty. *Journal of Advances in Modeling Earth Systems*, *11*(12), 4245–4287. https://doi.org/10.1029/2018ms001583

LeBauer, D. S., & Treseder, K. K. (2008). Nitrogen limitation of net primary productivity in terrestrial ecosystems is globally distributed. *Ecology*, *89*(2), 371–379. https://doi.org/10.1890/06-2057.1

Lehmann, J., Hansel, C. M., Kaiser, C., Kleber, M., Maher, K., Manzoni, S., et al. (2020). Persistence of soil organic carbon caused by functional complexity. *Nature Geoscience*, *13*(8), 529–534. https://doi.org/10.1038/s41561-020-0612-3

Lehmann, J., & Kleber, M. (2015). The contentious nature of soil organic matter. *Nature*, *528*(7580), 60–68. https://doi.org/10.1038/nature16069

Li, Z., Tian, D., Wang, B., Wang, J., Wang, S., Chen, H. Y. H., et al. (2019). Microbes drive global soil nitrogen mineralization and availability. *Global Change Biology*, *25*(3), 1078–1088. https://doi.org/10.1111/gcb.14557

Liang, C., Schimel, J. P., & Jastrow, J. D. (2017). The importance of anabolism in microbial control over soil carbon storage. *Nat Microbiol*, *2*(8), 17105. https://doi.org/10.1038/nmicrobiol.2017.105

Lipson, D. A., & Schmidt, S. K. (2004). Seasonal changes in an alpine soil bacterial community in the Colorado rocky mountains. *Applied and Environmental Microbiology*, *70*(5), 2867–2879. https://doi.org/10.1128/AEM.70.5.2867-2879.2004

Luo, Y. Q., Ahlstrom, A., Allison, S. D., Batjes, N. H., Brovkin, V., Carvalhais, N., et al. (2016). Toward more realistic projections of soil carbon dynamics by Earth system models. *Global Biogeochemical Cycles*, *30*(1), 40–56. https://doi.org/10.1002/2015gb005239

Manzoni, S., Čapek, P., Mooshammer, M., Lindahl, B. D., Richter, A., & Šantrůčková, H. (2017). Optimal metabolic regulation along resource stoichiometry gradients. *Ecology Letters*, *20*(9), 1182–1191. https://doi.org/10.1111/ele.12815

Meyerholt, J., & Zaehle, S. (2015). The role of stoichiometric flexibility in modelling forest ecosystem responses to nitrogen fertilization. *New Phytologist*, *208*(4), 1042–1055. https://doi.org/10.1111/nph.13547

Mooshammer, M., Wanek, W., Zechmeister-Boltenstern, S., & Richter, A. (2014). Stoichiometric imbalances between terrestrial decomposer communities and their resources: Mechanisms and implications of microbial adaptations to their resources. *Frontiers in Microbiology*, *5*, 22. https://doi.org/10.3389/fmicb.2014.00022

Nemergut, D. R., Cleveland, C. C., Wieder, W. R., Washenberger, C. L., & Townsend, A. R. (2010). Plot-scale manipulations of organic matter inputs to soils correlate with shifts in microbial community composition in a lowland tropical rain forest. *Soil Biology and Biochemistry*, *42*(12), 2153–2160. https://doi.org/10.1016/j.soilbio.2010.08.011

Parton, W. J., Schimel, D. S., Cole, C. V., & Ojima, D. S. (1987). Analysis of factors controlling soil organic-matter levels in Great-Plains grasslands. *Soil Science Society of America Journal*, *51*(5), 1173–1179. https://doi.org/10.2136/sssaj1987.03615995005100050015x

Parton, W. J., Scurlock, J. M. O., Ojima, D. S., Gilmanov, T. G., Scholes, R. J., Schimel, D. S., et al. (1993). Observations and modeling of biomass and soil organic matter dynamics for the grassland biome worldwide. *Global Biogeochemical Cycles*, *7*(4), 785–809. https://doi.org/10.1029/93GB02042

Pierson, D., Lohse, K. A., Wieder, W. R., Patton, N. R., Facer, J., de Graaff, M.-A., et al. (2022). Optimizing process-based models to predict current and future soil organic carbon stocks at high-resolution. *Scientific Reports*, *12*(1), 10824. https://doi.org/10.1038/s41598-022-14224-8

Poggio, L., de Sousa, L. M., Batjes, N. H., Heuvelink, G. B. M., Kempen, B., Ribeiro, E., & Rossiter, D. (2021). SoilGrids 2.0: Producing soil information for the globe with quantified spatial uncertainty. *SOIL*, *7*(1), 217–240. https://doi.org/10.5194/soil-7-217-2021

Polussa, A., Gonzalez-Rivero, J., Fields, N., Jevon, F. V., Wood, S. A., Wieder, W. R., & Bradford, M. A. (2021). Scale dependence in functional equivalence and difference in the soil microbiome. *Soil Biology and Biochemistry*, *163*, 108451. https://doi.org/10.1016/j.soilbio.2021.108451

Rocci, K. S., Barker, K. S., Seabloom, E. W., Borer, E. T., Hobbie, S. E., Bakker, J. D., et al. (2022). Impacts of nutrient addition on soil carbon and nitrogen stoichiometry and stability in globally-distributed grasslands. *Biogeochemistry*, *159*(3), 353–370. https://doi.org/10.1007/s10533-022-00932-w

Schimel, J. P. (2001). 1.13-Biogeochemical models: Implicit versus explicit microbiology. In M. H. Ernst-Detlef Schulze, S. Harrison, E. Holland, J. Lloyd, I. Colin Prentice, & D. S. Schimel (Eds.), *Global biogeochemical cycles in the climate system* (pp. 177–183). Academic Press.

Schimel, J. P., & Bennett, J. (2004). Nitrogen mineralization: Challenges of a changing paradigm. *Ecology*, *85*(3), 591–602. https://doi.org/10.1890/03-8002

Schimel, J. P., & Schaeffer, S. M. (2012). Microbial control over carbon cycling in soil. *Frontiers in Microbiology*, *3*, 348. https://doi.org/10.3389/fmicb.2012.00348

Serna-Chavez, H. M., Fierer, N., & van Bodegom, P. M. (2013). Global drivers and patterns of microbial abundance in soil. *Global Ecology and Biogeography*, *22*(10), 1162–1172. https://doi.org/10.1111/geb.12070

Shangguan, W., Dai, Y., Duan, Q., Liu, B., & Yuan, H. (2014). A global soil data set for earth system modeling. *Journal of Advances in Modeling Earth Systems*, *6*(1), 249–263. https://doi.org/10.1002/2013ms000293

Shi, Z., Crowell, S., Luo, Y., & Moore, B. (2018). Model structures amplify uncertainty in predicted soil carbon responses to climate change. *Nature Communications*, *9*(1), 2171. https://doi.org/10.1038/s41467-018-04526-9

Simpson, A. J., Simpson, M. J., Smith, E., & Kelleher, B. P. (2007). Microbially derived inputs to soil organic matter: Are current estimates too low? *Environmental Science & Technology*, *41*(23), 8070–8076. https://doi.org/10.1021/es071217x

Sokol, N. W., & Bradford, M. A. (2018). Microbial formation of stable soil carbon is more efficient from belowground than aboveground input. *Nature Geoscience*, *12*(1), 46–53. https://doi.org/10.1038/s41561-018-0258-6

Soong, J. L., Fuchslueger, L., Maranon-Jimenez, S., Torn, M. S., Janssens, I. A., Penuelas, J., & Richter, A. (2020). Microbial carbon limitation: The need for integrating microorganisms into our understanding of ecosystem carbon cycling. *Global Change Biology*, *26*(4), 1953–1961. https://doi.org/10.1111/gcb.14962

Sulman, B. N., Phillips, R. P., Oishi, A. C., Shevliakova, E., & Pacala, S. W. (2014). Microbe-driven turnover offsets mineral-mediated storage of soil carbon under elevated CO_2. *Nature Climate Change*, *4*(12), 1099–1102. https://doi.org/10.1038/nclimate2436

Sulman, B. N., Shevliakova, E., Brzostek, E. R., Kivlin, S. N., Malyshev, S., Menge, D. N. L., & Zhang, X. (2019). Diverse mycorrhizal associations enhance terrestrial C storage in a global model. *Global Biogeochemical Cycles*, *33*(4), 501–523. https://doi.org/10.1029/2018gb005973

Thomas, R. Q., Brookshire, E. N., & Gerber, S. (2015). Nitrogen limitation on land: How can it occur in earth system models? *Global Change Biology*, *21*(5), 1777–1793. https://doi.org/10.1111/gcb.12813

Thornton, P. E., Lamarque, J.-F., Rosenbloom, N. A., & Mahowald, N. M. (2007). Influence of carbon-nitrogen cycle coupling on land model response to CO_2 fertilization and climate variability. *Global Biogeochemical Cycles*, *21*(4), GB4018. https://doi.org/10.1029/2006gb002868

Thum, T., Caldararu, S., Engel, J., Kern, M., Pallandt, M., Schnur, R., et al. (2019). A new model of the coupled carbon, nitrogen, and phosphorus cycles in the terrestrial biosphere (QUINCY v1.0; revision 1996). *Geoscientific Model Development*, *12*(11), 4781–4802. https://doi.org/10.5194/gmd-12-4781-2019

Todd-Brown, K. E. O., Randerson, J. T., Post, W. M., Hoffman, F. M., Tarnocai, C., Schuur, E. A. G., & Allison, S. D. (2013). Causes of variation in soil carbon predictions from CMIP5 Earth system models and comparison with observations. *Biogeosciences*, *10*(3), 1717–1736. https://doi.org/10.5194/bg-10-1717-2013

van Groenigen, K. J., Qi, X., Osenberg, C. W., Luo, Y., & Hungate, B. A. (2014). Faster decomposition under increased atmospheric CO(2) limits soil carbon storage. *Science*, *344*(6183), 508–509. https://doi.org/10.1126/science.1249534

Wang, G., Huang, W., Zhou, G., Mayes, M. A., & Zhou, J. (2020). Modeling the processes of soil moisture in regulating microbial and carbon-nitrogen cycling. *Journal of Hydrology*, *585*, 124777. https://doi.org/10.1016/j.jhydrol.2020.124777

Wang, Y. P., Chen, B. C., Wieder, W. R., Leite, M., Medlyn, B. E., Rasmussen, M., et al. (2014). Oscillatory behavior of two nonlinear microbial models of soil carbon decomposition. *Biogeosciences*, *11*(7), 1817–1831. https://doi.org/10.5194/bg-11-1817-2014

Wang, Y. P., Law, R. M., & Pak, B. (2010). A global model of carbon, nitrogen and phosphorus cycles for the terrestrial biosphere. *Biogeosciences*, *7*(7), 2261–2282. https://doi.org/10.5194/bg-7-2261-2010

Wang, Y. P., Zhang, H., Ciais, P., Goll, D., Huang, Y., Wood, J. D., et al. (2021). Microbial activity and root carbon inputs are more important than soil carbon diffusion in simulating soil carbon profiles. *Journal of Geophysical Research: Biogeosciences*, *126*(4), e2020JG006205. https://doi.org/10.1029/2020jg006205

Wardle, D. A., Bardgett, R. D., Klironomos, J. N., Setala, H., van der Putten, W. H., & Wall, D. H. (2004). Ecological linkages between aboveground and belowground biota. *Science*, *304*(5677), 1629–1633. https://doi.org/10.1126/science.1094875

Whalen, E. D., Grandy, A. S., Sokol, N. W., Keiluweit, M., Ernakovich, J., Smith, R. G., & Frey, S. D. (2022). Clarifying the evidence for microbial- and plant-derived soil organic matter, and the path toward a more quantitative understanding. *Global Change Biology*, *28*(24), 7167–7185. https://doi.org/10.1111/gcb.16413

Wieder, W. R., Bonan, G. B., & Allison, S. D. (2013). Global soil carbon projections are improved by modelling microbial processes. *Nature Climate Change*, *3*(10), 909–912. https://doi.org/10.1038/nclimate1951

Wieder, W. R., Cleveland, C. C., Smith, W. K., & Todd-Brown, K. (2015). Future productivity and carbon storage limited by terrestrial nutrient availability. *Nature Geoscience*, *8*(6), 441–444. https://doi.org/10.1038/ngeo2413

Wieder, W. R., Grandy, A. S., Kallenbach, C. M., & Bonan, G. B. (2014). Integrating microbial physiology and physio-chemical principles in soils with the MIcrobial-MIneral Carbon Stabilization (MIMICS) model. *Biogeosciences*, *11*(14), 3899–3917. https://doi.org/10.5194/bg-11-3899-2014

Wieder, W. R., Grandy, A. S., Kallenbach, C. M., Taylor, P. G., & Bonan, G. B. (2015). Representing life in the Earth system with soil microbial functional traits in the MIMICS model. *Geoscientific Model Development*, *8*(6), 1789–1808. https://doi.org/10.5194/gmd-8-1789-2015

Wieder, W. R., & Hartman, M. (2023). Global MIMICS-CN from biogeochemical testbed (Version 1.0) [Dataset]. *UCAR/NCAR-GDEX*. https://doi.org/10.5065/jqts-cg20

Wieder, W. R., Hartman, M. D., Sulman, B. N., Wang, Y.-P., Koven, C. D., & Bonan, G. B. (2018). Carbon cycle confidence and uncertainty: Exploring variation among soil biogeochemical models. *Global Change Biology*, *24*(4), 1563–1579. https://doi.org/10.1111/gcb.13979

Wieder, W. R., Sulman, B. N., Hartman, M. D., Koven, C. D., & Bradford, M. A. (2019). Arctic soil governs whether climate change drives global losses or gains in soil carbon. *Geophysical Research Letters*, *46*(24), 14486–14495. https://doi.org/10.1029/2019gl085543

will wieder, & melanniehartman. (2023). *wwieder/biogeochem_testbed: v2.0.0 (Testbed-CN)*. Zenodo. https://doi.org/10.5281/zenodo.7636495

Xu, X., Thornton, P. E., & Post, W. M. (2013). A global analysis of soil microbial biomass carbon, nitrogen and phosphorus in terrestrial ecosystems. *Global Ecology and Biogeography*, *22*(6), 737–749. https://doi.org/10.1111/geb.12029

Xu, X., Thornton, P. E., & Potapov, P. (2014). A compilation of global soil microbial biomass carbon, nitrogen, and phosphorus data (version) [Dataset]. *Oak Ridge, Tennessee, USA*. https://doi.org/10.3334/ORNLDAAC/1264

Yang, X., Ricciuto, D. M., Thornton, P. E., Shi, X., Xu, M., Hoffman, F., & Norby, R. J. (2019). The effects of phosphorus cycle dynamics on carbon sources and sinks in the amazon region: A modeling study using ELM v1. *Journal of Geophysical Research: Biogeosciences*, *124*(12), 3686–3698. https://doi.org/10.1029/2019jg005082

Yue, K., Fornara, D. A., Yang, W., Peng, Y., Li, Z., Wu, F., & Peng, C. (2017). Effects of three global change drivers on terrestrial C:N:P stoichiometry: A global synthesis. *Global Change Biology*, *23*(6), 2450–2463. https://doi.org/10.1111/gcb.13569

Zaehle, S., Friedlingstein, P., & Friend, A. D. (2010). Terrestrial nitrogen feedbacks may accelerate future climate change. *Geophysical Research Letters*, *37*(1), L01401. https://doi.org/10.1029/2009gl041345

Zaehle, S., Jones, C. D., Houlton, B., Lamarque, J. F., & Robertson, E. (2015). Nitrogen availability reduces CMIP5 projections of twenty-first-century land carbon uptake. *Journal of Climate*, *28*(6), 2494–2511. https://doi.org/10.1175/Jcli-D-13-00776.1

Zechmeister-Boltenstern, S., Keiblinger, K. M., Mooshammer, M., Peñuelas, J., Richter, A., Sardans, J., & Wanek, W. (2015). The application of ecological stoichiometry to plant–microbial–soil organic matter transformations. *Ecological Monographs*, *85*(2), 133–155. https://doi.org/10.1890/14-0777.1

Zhang, H., Goll, D. S., Wang, Y.-P., Ciais, P., Wieder, W. R., Abramoff, R., et al. (2020). Microbial dynamics and soil physicochemical properties explain large-scale variations in soil organic carbon. *Global Change Biology*, *26*(4), 2668–2685. https://doi.org/10.1111/gcb.14994

Zhang, Y., Lavallee, J. M., Robertson, A. D., Even, R., Ogle, S. M., Paustian, K., & Cotrufo, M. F. (2021). Simulating measurable ecosystem carbon and nitrogen dynamics with the mechanistically defined MEMS 2.0 model. *Biogeosciences*, *18*(10), 3147–3171. https://doi.org/10.5194/bg-18-3147-2021

Zhu, Q., Riley, W. J., Tang, J., Collier, N., Hoffman, F. M., Yang, X., & Bisht, G. (2019). Representing nitrogen, phosphorus, and carbon interactions in the E3SM land model: Development and global benchmarking. *Journal of Advances in Modeling Earth Systems*, *11*(7), 2238–2258. https://doi.org/10.1029/2018ms001571